Report 78-2 March 1978

# RADAR ECHO PATTERNS IN NORTH DAKOTA AND IMPLICATIONS FOR THE DESIGN OF RAIN GAGE NETWORKS TO SUPPORT OPERATIONAL RADAR RAINFALL MEASUREMENT

By: Robert W. Dixon and Paul L. Smith, Jr.

Prepared for:

NOAA/National Weather Service
Gramax Building
8060 13th Street
Silver Spring, MD 20910

Contract No. 5-35376

Institute of Atmospheric Sciences

South Dakota School of Mines and Technology

Rapid City, South Dakota 57701

Report 78-2 March 1978

# RADAR ECHO PATTERNS IN NORTH DAKOTA AND IMPLICATIONS FOR THE DESIGN OF RAIN GAGE NETWORKS TO SUPPORT OPERATIONAL RADAR RAINFALL MEASUREMENT

By: Robert W. Dixon and Paul L. Smith, Jr.

Prepared for:

NOAA/National Weather Service
Gramax Building
8060 13th Street
Silver Spring, MD 20910

Contract No. 5-35376

Institute of Atmospheric Sciences

South Dakota School of Mines and Technology

Rapid City, South Dakota 57701

# FOREWORD

This report constitutes one volume of the final report under Contract No. 5-35376. Initially the report was drafted in the form of an M.S. thesis by Robert W. Dixon. That draft was reworked by Dr. Smith into the present form in order to make the results available to interested scientists. As of the date of printing of this report, the final version of the thesis has not been completed and defended.

## ABSTRACT

A study was made of the precipitation patterns obtained from digital recordings of radar echoes from one summer's rainfall in North Dakota. The data were analyzed to yield frequency distributions of the percentage of the total radar surveillance area covered by echoes. Median coverages obtained for accumulation time intervals of one scan, one hour, two hours, and three hours were 1.1%, 4.5%, 6.8%, and 8.7%, respectively.

Using those frequency distributions, the probabilities that some radar echo would hit at least one gage in a randomly distributed rain gage network during a given time interval were generated. For example, in a three-hour interval the probability that some radar echo would pass over at least one rain gage in a 30-gage random network was found to be only 74%. This suggests that for the numbers of gages that are reasonable to consider for a real-time automated reporting network, there will be very few rain events reported in the time intervals of interest. To obtain more realistic frequencies of such "radar rain events," symmetrical gage networks were designed in both triangular and rectangular grid formats. The relative frequencies of events were then determined by passing (through computer simulation) the entire summer's echo data over them. The results were surprisingly similar to those obtained for the random networks, suggesting that for the numbers of gages considered the events are essentially independent. One common feature of the results is that beyond a network size of about 20 to 30 gages, the frequencies of events increase very slowly.

For any adjustment of radar rainfall estimates to be made, it is imperative to have some rain gage data. To determine the proper network size, gage placement, and data collection time interval, an acceptable level of the frequency of reported events must first be decided upon. The results of this study give estimates of the frequencies of events obtainable with different combinations and thus offer guidance as to the kind of gage network needed to support operational adjustment of radar rainfall estimates.

TABLE OF CONTENTS

TABLE OF CONTENTS (Continued)

# LIST OF FIGURES

LIST OF FIGURES (Continued)

# LIST OF TABLES

# 1. INTRODUCTION

## 1.1 Requirements for Rain Gage Data to Adjust Radar Rainfall Estimates in Real Time

There have been many studies comparing gage and radar estimates of rainfall amounts. Experiments have been conducted to determine the gage network density required to measure rainfall directly or to support adjustments of the radar reflectivity factor - rainfall rate (Z-R) relationship. Various approaches have been taken in the design of the gage networks, such as grouping the gages or setting them in a symmetrical grid.

Once the investigation leaves the experimental mode and enters an operational one, additional problems begin to show up. Operationally, the only way to obtain rain gage reports in real time will be to set up a telemetering rain gage network. Due to the expense of each such gage, the monetary requirements to form an extensive network would be enormous. This makes the use of radar attractive for real-time measurements of rainfall amounts over watershed areas. To give adequate confidence in the radar data, however, some comparisons with rain gage measurements are usually required. With only sparse telemetering rain gage networks available, the problem becomes one of acquiring enough rain gage events to serve as a basis for evaluating the radar rainfall estimates. Here we define a "rain gage event" as the occurrence at a gage location of an amount of rain sufficient to be usable in making a comparison with radar estimates.

The main question this report deals with is, "For a given rain gage network size, how many rain gage events are likely to occur during a given time interval?" To deal with this question, a study was made of the patterns of a summer's rainfall observed by radar in North Dakota. Using the radar data tapes of the 1972 North Dakota Pilot Project (Smith et al., 1975), frequency distributions of echo area coverage were generated for different time intervals and reflectivity factor thresholds. From this set of values, probabilities of obtaining rain gage events were computed for varying numbers of rain gages (60 gages being the limit) in randomly placed networks. Detailed computer simulations were then made by passing the entire summer's precipitation echo data over symmetrical triangular and rectangular rain gage networks of varying densities. The relative frequencies of various sets of gage events were determined from these simulations. As different suitability criteria might be established for events to be used in operational evaluation or adjustment of the radar rainfall estimates, different thresholds of rain amounts and numbers of events were considered in the simulations.

The final results of this study offer basic guideline information on the rain gage networks required to provide gage data adequate for making operational adjustments of the radar rainfall estimates.

## 1.2 Background of the Problem

Several earlier studies considered the gage requirements to support adjustment of radar rainfall estimates. Some studies conclude that the required gage density is very great, while others suggest that satisfactory results can be obtained with sparse networks. Recently Woodley et al. (1974, 1975) used for the Florida Area Cumulus Experiment (FACE) target area in Florida an approach involving small areas with dense rain gage groupings (called clusters). They found significant variability in the rainfall amounts collected by rain gages, no matter how dense the network. Differences for nearby gages varied between 5 and 12% for maximum rainfall amounts of 0.1 inch (2.54 mm) to 1.0 inch (25.4 mm). Because of this variability, Woodley et al. clustered several rain gages so a reasonable sampling of rainfall amounts could be obtained to adjust the radar estimated rainfall for the same and nearby areas. They found that this adjustment improved the comparison between gage and radar estimates for the FACE MESONET (an independent, less dense gage network covering a larger sampling area). In their conclusion, Woodley et al. suggested that the gaging requirement for adjustment of radar estimates of rainfall over an area of 4,000 $mi^2$ (13,000 $km^2$) would be about 40 gages arranged into several clusters of 7 to 10 gages each.

Huff (1969, 1970) presented a rainfall climatology obtained by the Illinois State Water Survey that provided results using only rain gage networks to determine areal rainfall. As expected, a very dense network is required to obtain reliable information consistently. In Fig. 1, Huff suggests a power law relation between the size of the sampling area and the gage density required to detect storms. The gage density requirements in Fig. 1 depend on three criteria, the first being the sampling area; the second, the amount of rainfall to be detected; and the third, the percentage of storms to be detected. In an earlier study, Huff (1967) had concluded that a very dense gage network would be required to serve as a basis for adjusting radar rainfall estimates in Illinois. For Huff's conclusions to be applied to an operational project of sizable sampling area, an enormous gage network would have to be established.

Contrasting results were obtained by Brandes (1975), who showed that with data from a few rain gages used to adjust the radar rainfall estimates, the differences between gage and radar estimates at other locations were reduced significantly. Brandes found that when the adjusting gage density was increased by approximately a factor 2 [from 1600 $mi^2$/gage (4300 $km^2$/gage) to 900 $mi^2$/gage (2330 $km^2$/gage)],

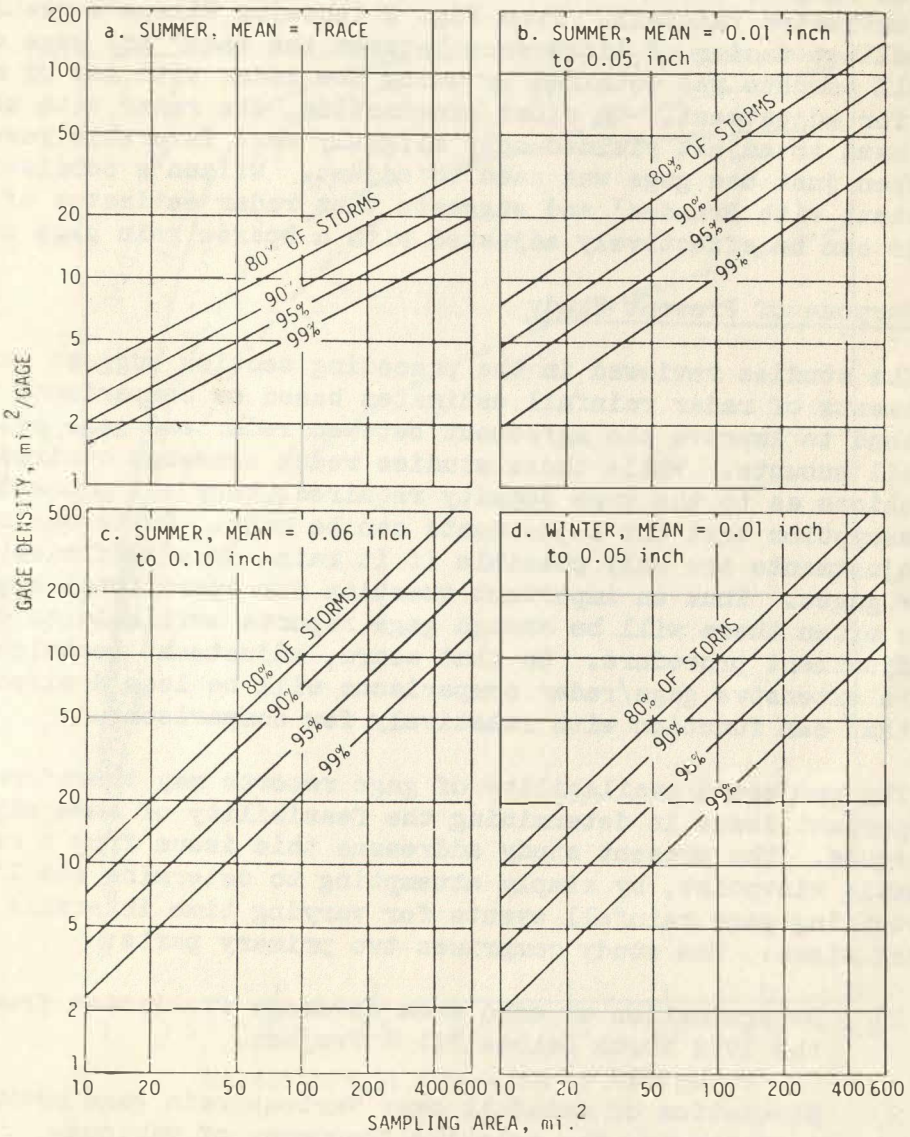


***Fig. 1.*** **Sampling requirements for precipitation detection by rain gages. Grouped by seasons and mean precipitation. (From Huff, 1969)**

the estimated differences decreased by only 1%. Consequently, Brandes inferred that the rain gage networks do not have to be dense in order to adjust the radar rainfall estimates.

A similar conclusion came earlier from Wilson (1970), who tested the idea of using sparse rain gage networks [1000 $mi^2$/gage (2600 $km^2$/gage)] with several different techniques to adjust the radar estimated rainfall. From Fig. 2 (showing Wilson's results), the smallest factor of difference between the radar and gage estimated rainfall amounts was obtained by using the radar with one or more gages for adjustment. On close examination, the radar with three gages used to adjust yielded only slightly more favorable results than when just one gage was used to adjust. Wilson's conclusion is consistent with Brandes' and suggests that radar estimates of rainfall amounts can be effectively adjusted with a sparse rain gage network.

## 1.3 Purpose of Present Study

The studies reviewed in the preceding section suggest that adjustments of radar rainfall estimates based on comparisons with gage data tend to improve the agreement between radar and gage estimates of rainfall amounts. While those studies reach somewhat contradictory conclusions as to the gage density required, they all proceed from the assumption that the adjustments can be made. Quite obviously, the adjustments are only possible if it rains on a sufficient number of the gages. Thus an important question for operational applications is how often there will be enough gage reports available to carry out the adjustment procedure. On that score, adjustment techniques which require extensive gage/radar comparisons will be less desirable than ones that can function with relatively few comparisons.

The projected availability of gage reports may therefore become an important issue in determining the feasibility of some adjustment techniques. The present study addresses this issue from a rather pragmatic viewpoint, by simply attempting to determine the likelihood of obtaining gage rainfall events for varying time intervals and gage network sizes. The study comprises two primary parts:

1) Determination of echo area coverage statistics from the 1972 North Dakota Pilot Project.

2) Simulation of rainfall over various rain gage networks to determine the relative frequency of various combinations of gage events.

In a real-time system, the utility of some approaches may ultimately be decided by the availability of gage reports.

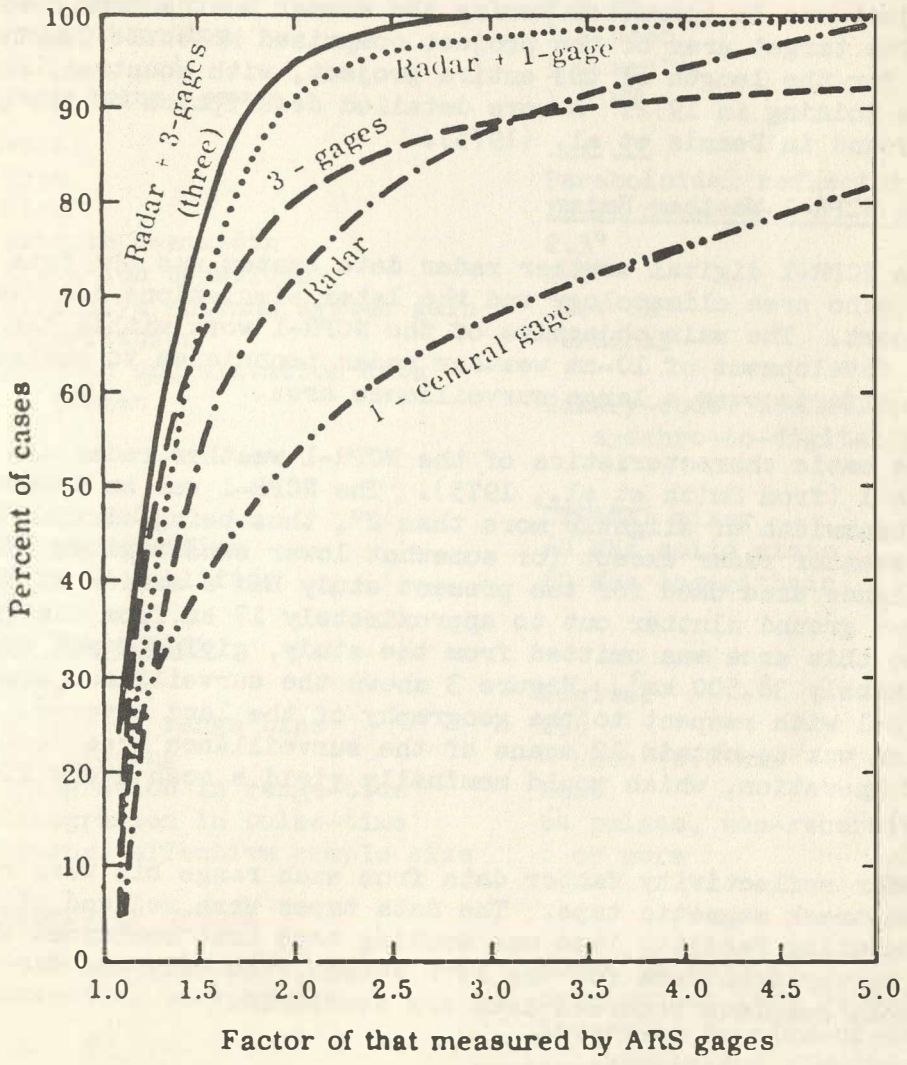


*Fig. 2.* Percentage of storm total rainfall estimates within the indicated factor of difference between radar and/or rain gages and the Agricultural Research Service rain gage network. The sampling area was 1000 $mi^2$ ($\approx$26,000 $km^2$) near Chickasha, Oklahoma. (From Wilson, 1970)

# 2. DATA BASE

## 2.1 The North Dakota Pilot Project

The North Dakota Pilot Project (NDPP) was a randomized cloud seeding experiment studying weather modification techniques in the northern Great Plains. Headquartered in Watford City, North Dakota, the project was in operation during the summer months from 1969 through 1972. The target area of the project comprised McKenzie County, North Dakota, for the length of the entire project, with Mountrail and Ward counties joining in 1972. A more detailed description of the project may be found in Dennis et al. (1975).

## 2.2 The NCPR-1 Weather Radar

The NCPR-1 digital weather radar data system was the data source for the echo area climatology and the later simulations discussed in this report. The main objective of the NCPR-1 work within the NDPP was the development of 10-cm weather radar techniques to analyze cloud seeding efforts over a large surveillance area.

The basic characteristics of the NCPR-1 weather radar are given in Table 1 (from Smith et al., 1975). The NCPR-1 was an S-band system with a beamwidth of slightly more than 2°, thus being similar to the WSR-57 weather radar except for somewhat lower sensitivity. The radar surveillance area used for the present study had a radius of 112 km. There was ground clutter out to approximately 17 km from the radar site, so this area was omitted from the study, giving a net area of approximately 38,500 $km^2$. Figure 3 shows the surveillance area of the NCPR-1 with respect to the geography of the land covered. The intention was to obtain 12 scans of the surveillance area during each hour of operation, which would nominally yield a scan every five minutes.

Radar reflectivity factor data from each range bin were recorded on seven-track magnetic tape. The data tapes were reduced at the NCAR Computing Facility into one working tape that contained the entire survey scan data for the 1972 season, the only one for which reasonably complete recorded data are available.

## 2.3 1972 Summer Field Operations

The 1972 North Dakota Pilot Project field season began on 16 May and continued until 31 August. The project headquarters near Watford City was also the base for the NCPR-1 weather radar.

*TABLE 1:* Characteristics of the NCPR-1 weather radar data system (from Smith et al., 1975)

| | |
|---|---|
| **A. Radar Set** | |
| Transmitter: | |
| Basic type | Nike-Ajax acquisition (magnetron) |
| Wavelength | 9.4 cm |
| Pulse duration | 1.3 μsec |
| PRF | 500 $sec^{-1}$ |
| Peak trans. power | 1.0 MW |
| Antenna: | |
| Type | Paraboloidal reflector |
| Size | 10 ft diameter |
| Azimuth beamwidth | 2.3° |
| Elevation beamwidth | 2.6° |
| Effective antenna system gain | 34.4 dB |
| Polarization | Vertical |
| Azimuth and elevation data format | Binary-coded decimal (optical synchro-to-digital converters) |
| Receiver: | |
| Front end | Crystal mixer |
| IF preamplifier | 60 MHz solid state |
| Main IF amplifier | 60 MHz logarithmic |
| **B. Video Integrator** | |
| Type | Digital |
| Number of range bins | 256 |
| Bin spacing | 4 μsec (0.6 km) |
| Integration in range-time | None |
| Integration in pulse-time | 64 pulses, non-recursive |
| Approx. effective sample size | 6 or more |
| **C. Minicomputer System** | |
| Basic computer CPU | Nova (8K memory) |
| Essential peripherals | Synchronous tape recorder<br>Interface to time-of-day clock, azimuth and elevation shaft encoders, and azimuth and elevation servos<br>Storage display/scan converter |
| Data Grid: | |
| Coordinate system | Azimuth-elevation-range |
| Azimuth resolution | 2.0° |
| Elevation resolution | 2.0° |
| Range resolution | 0.6 km |
| Reflectivity factor resolution | 1.3 dB approx. |

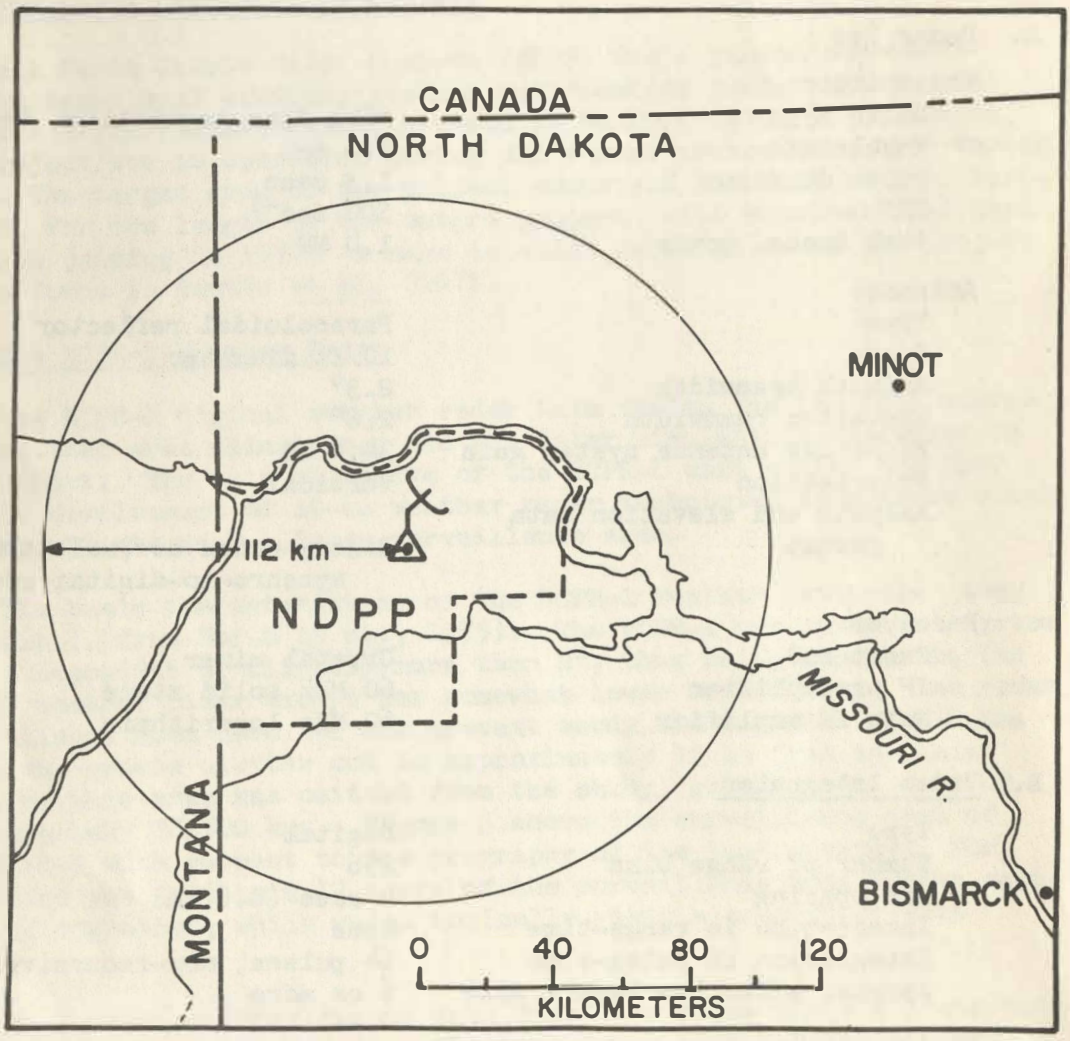


*Fig. 3.* Map showing the location of the North Dakota Pilot Project area centered at the Watford City radar site. The region within the 112 km radar surveillance radius was the source of the radar echo data used for the radar climatology study.

The operational day was 12 hours long, beginning at 1000 CDT. The NCPR-1 was not operated continuously, but became operational when precipitation was detected by an M-33 weather radar (which also was in use for the project), or by visual observation from the area. Of the 1248 total possible hours of the project, the NCPR-1 recorded 320 hours of data, which came to approximately 26% of the time in operation. The radar observations were supported by a network of 126 conventional and 22 recording rain gages, but we shall not be concerned with those data here. A summary of the 1972 North Dakota Pilot Project's operation can be found in Miller and Cain (1973).

# 3. RADAR CLIMATOLOGY STUDIES

As an indication of the expected frequency of gage events in a specific radar surveillance area, a climatology of the radar echo area coverage is useful. The frequency distributions of echo coverage in North Dakota were therefore studied. The results were then compared against previous echo climatology studies in other areas.

For this study, four different time intervals were examined with respect to echo area coverage. In order, with respect to the data accumulation times of the NCPR-1, they are:

1. "Instantaneous" - 360° azimuth survey scan at elevation 2°; nominally one scan every 5 minutes.

2. "One-Hour" - one-hour clock intervals beginning at 1000 CDT and every one hour thereafter.

3. "Two-Hour" - two-hour clock intervals beginning at 1000 CDT and every 2 hours thereafter.

4. "Three-Hour" - three-hour clock intervals beginning at 1000 CDT and incremented every 3 hours thereafter.

The starting data times for respective time intervals do not overlap; for example, the beginning times for three-hour intervals for a sample day would be 1000, 1300, 1600, and 1900 CDT.

## 3.1 Cumulative Frequency Distributions of Echo Area Coverage

Cumulative frequency distributions were constructed for the respective time intervals to give an idea of the fraction of the radar surveillance area covered with echoes when precipitation is present. Bunting and Conover (1971) referred to this fraction, expressed in percentage terms, as the "Radar Index." For these frequency distributions, there were 3146, 337, 196, and 145 instantaneous, one-hour, two-hour, and three-hour time intervals, respectively, with some radar echo in the surveillance area at some time during the specified interval. Intervals during which no echoes appeared were not counted in this analysis.

Figure 4 presents the cumulative frequency distributions of echo area coverage, with the time interval as a parameter. In determining these distributions, a "point" (radar range bin) was counted if some echo was present at any time during the interval. As expected, the

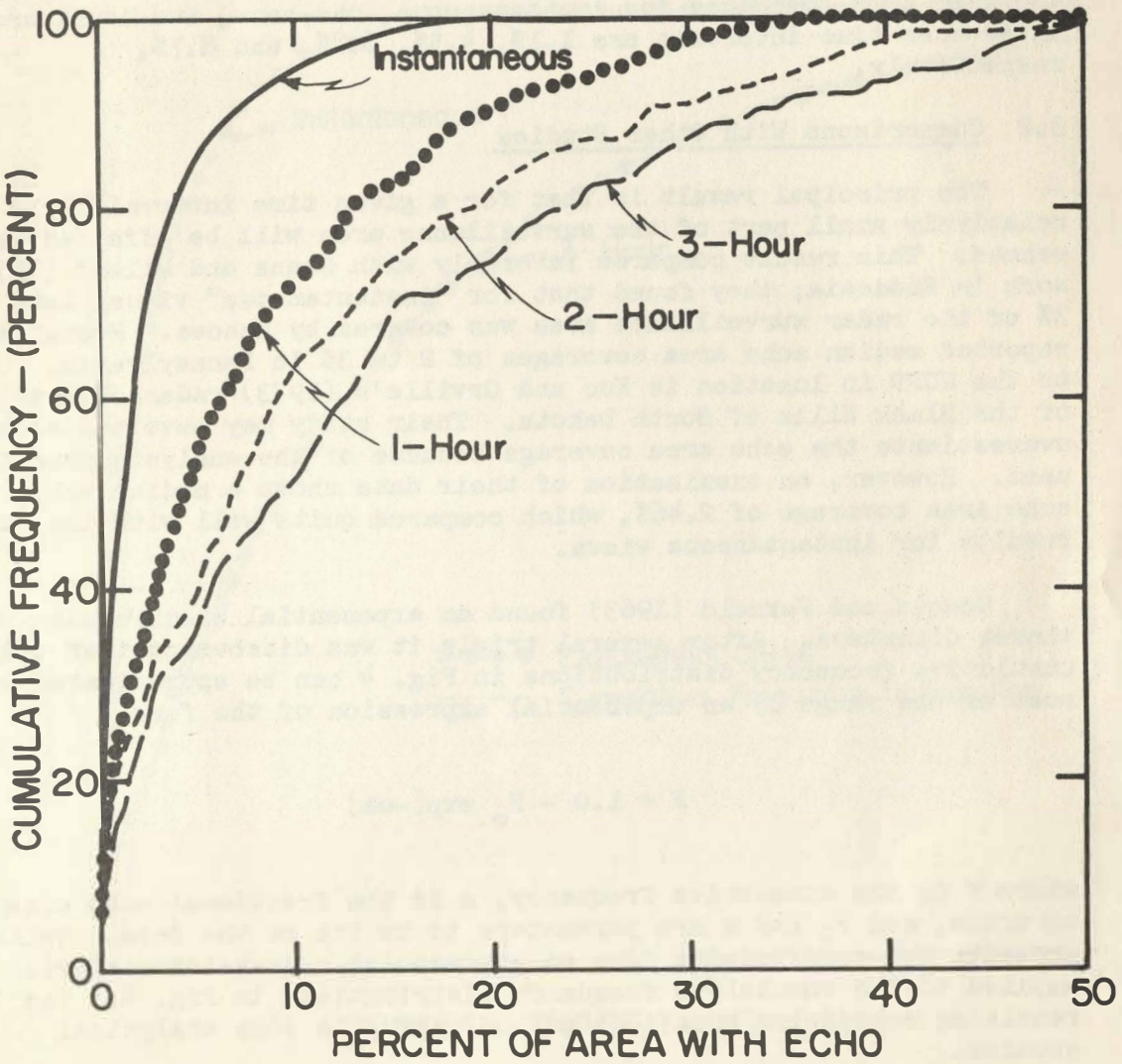


*Fig. 4.* The cumulative frequency distribution of echo area coverage with data accumulation time interval as a parameter. The data are from the 1972 North Dakota Pilot Project summer operation gathered on the NCPR-1 weather radar. Only situations with some echo present in the surveillance area were counted in the analysis.

area coverages increase for longer time intervals; however, it is remarkable that the echo area coverage is so small when even three-hour intervals are considered. For example, at the 50% cumulative frequency (which represents the median value for the distributions), the echo area coverages for instantaneous, one-hour, two-hour, and three-hour time intervals are 1.1%, 4.5%, 6.8%, and 8.7%, respectively.

### 3.2 Comparisons With Other Studies

The principal result is that for a given time interval, only a relatively small part of the surveillance area will be affected by echoes. This result compares favorably with Soane and Miles' (1955) work in Rhodesia; they found that for "instantaneous" views, less than 3% of the radar surveillance area was covered by echoes. Myers (1964) reported median echo area coverages of 2 to 3% in Pennsylvania. Closer to the NDPP in location is Kuo and Orville's (1973) radar climatology of the Black Hills of South Dakota. Their study may have tended to overestimate the echo area coverage because of the analysis procedure used. However, an examination of their data shows a median value for echo area coverage of 2.46%, which compares quite well with the other results for instantaneous views.

Dennis and Fernald (1963) found an exponential distribution for shower diameters. After several trials it was discovered that the cumulative frequency distributions in Fig. 4 can be approximated over most of the range by an exponential expression of the form

$$F = 1.0 - F_o \exp[-\alpha a] \qquad (1)$$

where F is the cumulative frequency, a is the fractional echo area coverage, and $F_o$ and $\alpha$ are parameters to be fit to the data. Table 2 presents the coefficients from an exponential regression analysis applied to the cumulative frequency distributions in Fig. 4. The resulting regression equations may be useful in some analytical studies.

A comparison of the exponential equations to the actual cumulative frequency distributions can be found in Fig. 5, where the instantaneous and three-hour time intervals are used as examples. The regression equations are somewhat deficient in representing the cumulative frequency distributions for small and very large echo coverage areas, but otherwise fit the observations quite closely.

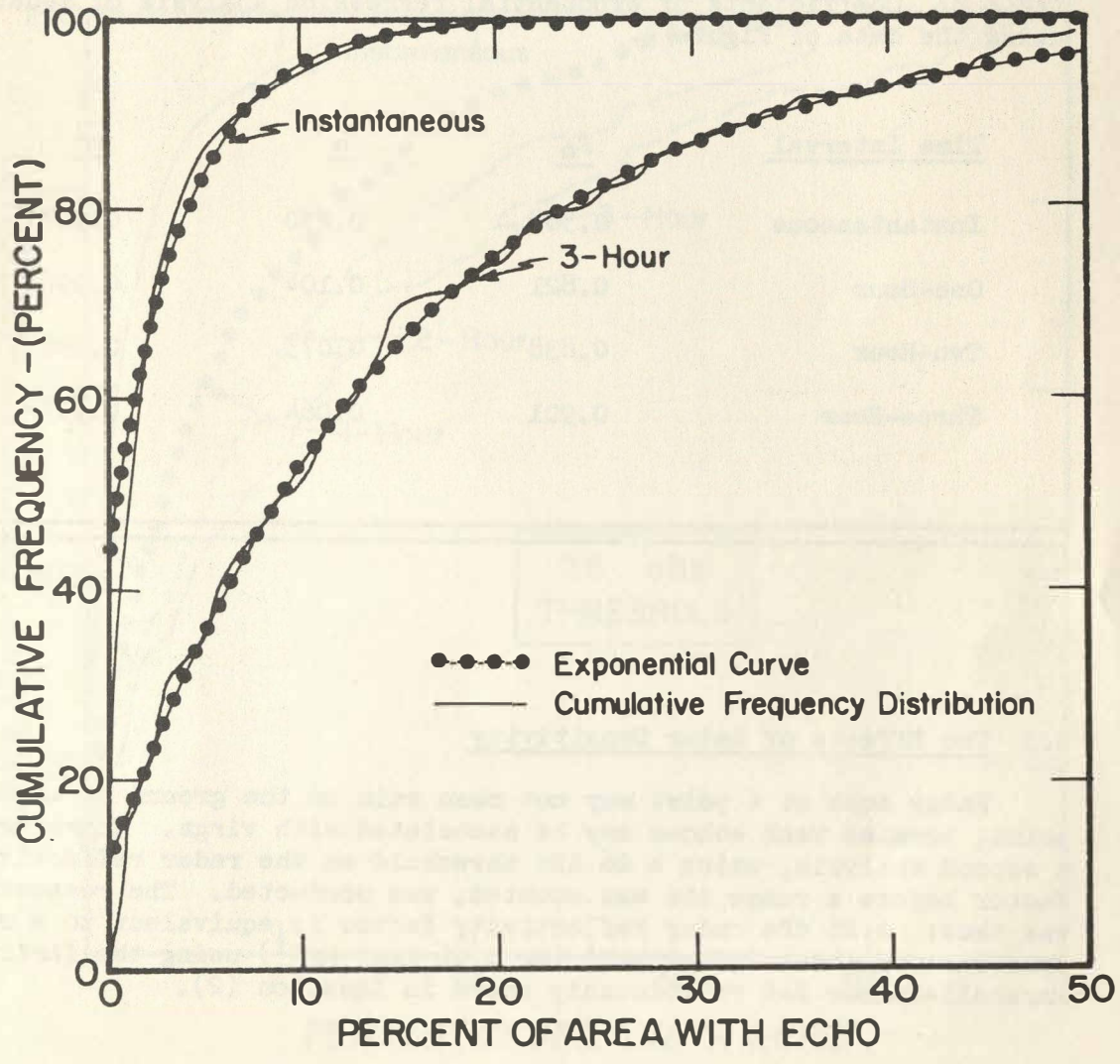


*Fig. 5.* The exponential relation $F = 1.0 - F_0 \exp[-\alpha a]$ compared with the cumulative frequency distributions (Fig. 4) used in the regression analysis, for instantaneous and 3-hour time intervals. The regression coefficients can be found in Table 2.

*TABLE 2:* Coefficients of exponential regression analysis of Equation (1) using the data of Figure 4.

| Time Interval | $F_o$ | $a$ | $r^2$ |
|---|---|---|---|
| Instantaneous | 0.588 | 0.250 | 0.968 |
| One-Hour | 0.821 | 0.104 | 0.996 |
| Two-Hour | 0.838 | 0.075 | 0.996 |
| Three-Hour | 0.901 | 0.064 | 0.997 |

### 3.3 The Effects of Radar Sensitivity

Radar echo at a point may not mean rain on the ground at that point, because weak echoes may be associated with virga. Therefore, a second analysis, using a 26 dBz threshold on the radar reflectivity factor before a range bin was counted, was conducted. The reasoning was thus: A 26 dBz radar reflectivity factor is equivalent to a rainfall rate of about 1.5 mm $hr^{-1}$ (or 0.06 inch $hr^{-1}$) using the familiar Marshall-Palmer Z-R relationship shown in Equation (2).

$$Z\ (\text{dBz}) = 23 + 16 \log[R/(1\ \text{mm hr}^{-1})] \qquad (2)$$

If a 26 dBz echo appeared at a point on two successive scans, the rainfall estimated would be about 0.25 mm (0.01 inch), enough to be measurable by a gage.

The cumulative frequency distributions were recomputed with this 26 dBz reflectivity threshold. Figure 6 shows the results, which can be compared to the distributions without any restriction (Fig. 4).

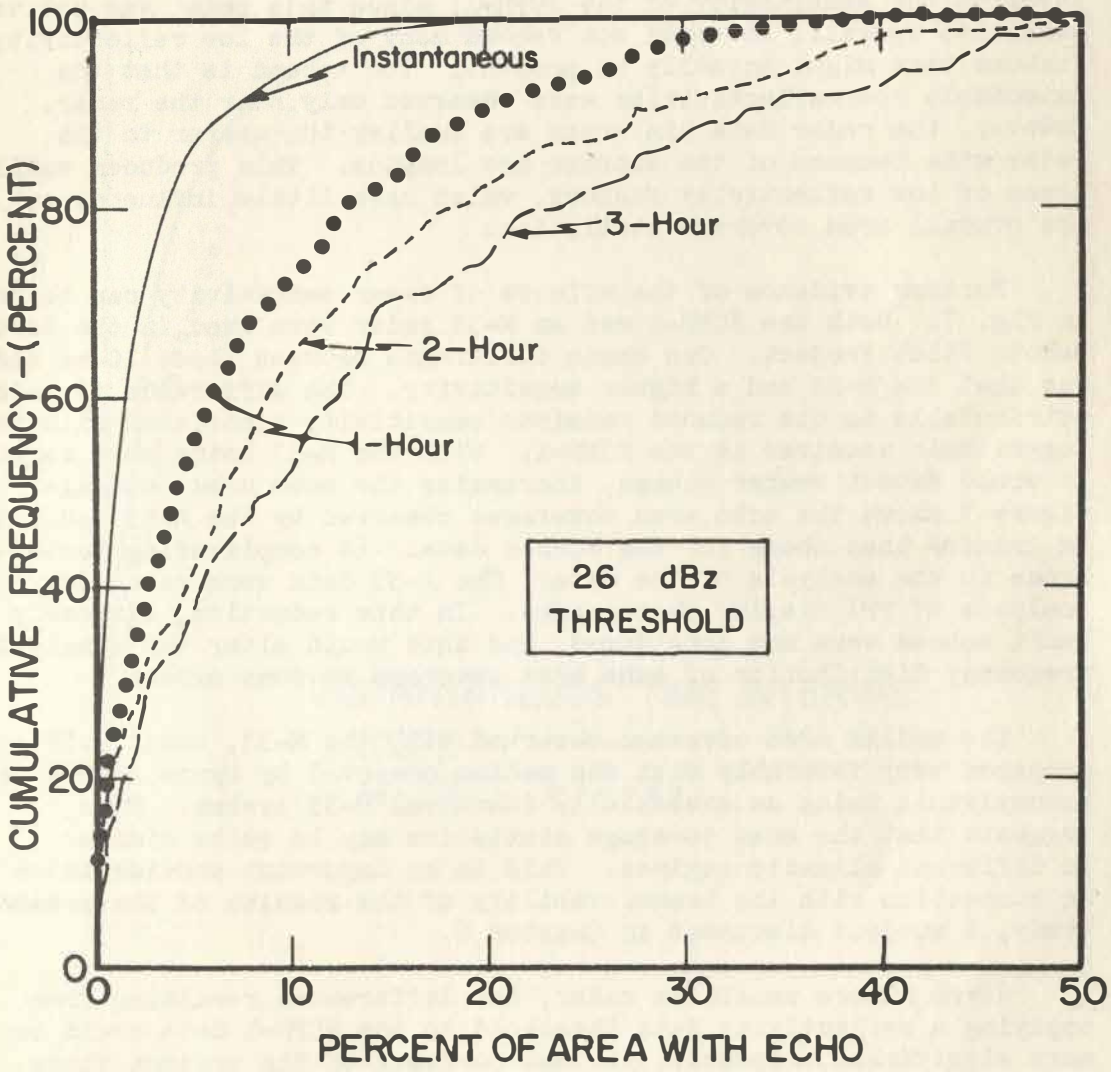


*Fig. 6.* Cumulative frequency distributions of echo area coverage with data accumulation time interval as a parameter. Echoes were required to have a reflectivity factor of ≥26 dBz before being counted.

Although the NCPR-1 could detect nearby echoes as weak as 12 dBz, the analysis with the 26 dBz restriction gave almost identical results. There are two possible explanations for this occurrence. The first involves the sensitivity of the NCPR-1; since this radar was not very sensitive overall, it would not record many of the low reflectivity factors that might actually be present. The second is that the detectable low reflectivities were observed only near the radar. However, the radar data bin areas are smaller the nearer to the radar site because of the shorter arc lengths. This produces small areas of low reflectivity factors, which have little influence on the overall area coverage statistics.

Further evidence of the effects of radar sensitivity can be seen in Fig. 7. Both the NCPR-1 and an M-33 radar were used in the North Dakota Pilot Project. One basic difference between these 10-cm radars was that the M-33 had a higher sensitivity. The difference is mainly attributable to the reduced receiver sensitivity associated with the logarithmic receiver in the NCPR-1. With the M-33 being more sensitive, it would detect weaker echoes, increasing the echo area coverage. Figure 7 shows the echo area coverages observed by the M-33 radar to be greater than those for the NCPR-1 data. (A complicating factor arose in the analysis of the data: The M-33 data were reduced by analysis of PPI display photographs. In this reduction, extremely small echoes were not considered, and this would alter the cumulative frequency distribution of echo area coverage to some extent.)

The median area coverage observed with the M-33, about 2.5%, compares very favorably with the median observed by Myers (1964) in Pennsylvania using an essentially identical M-33 system. This suggests that the area coverage statistics may be quite similar in different climatic regimes. This is an important consideration in connection with the transferability of the results of the present study, a subject discussed in Chapter 6.

Given a more sensitive radar, the differences resulting from applying a reflectivity data threshold to the NCPR-1 data could be more significant. However, for the purposes of the present study, the 26 dBz threshold was eliminated from further investigations because of the small change of the results compared to those obtained with no restrictions.

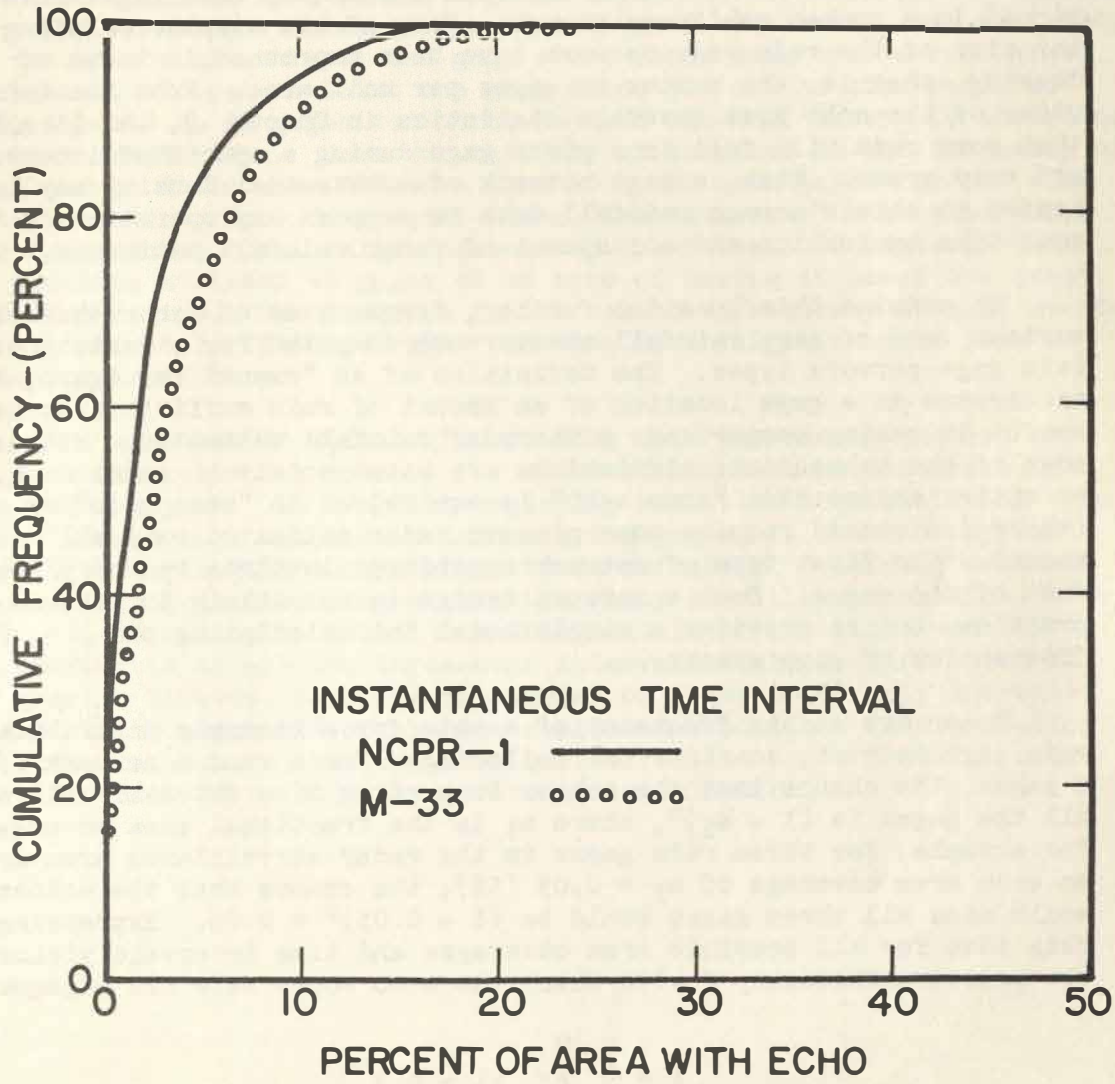


*Fig. 7.* Cumulative frequency distributions of echo area coverage in 1972, as viewed from the Watford City, North Dakota, radar site by two different 10-cm radar sets. The NCPR-1 data represent scans made at nominal 5-min intervals and were recorded and analyzed by digital techniques. The M-33 data were reduced manually from PPI photographs taken at 15-minute intervals. In both cases, only situations with some echo present were counted.

## 4. FREQUENCIES OF GAGE EVENTS FOR RANDOMLY DISTRIBUTED NETWORKS

For most studies of radar rainfall estimates, rain gages have been placed in a rather arbitrary manner. Many of the results relating to the size of the rain gage network have been expressed in terms of density, that is, the number of gages per unit area. From the indications of the echo area coverage statistics in Chapter 3, the likelihood that some rain will fall in a given gage during a specified interval is not very great. Thus, a gage network of substantial density may be needed to obtain enough rainfall data to support any operational real-time evaluation and adjustment of radar rainfall estimates.

To examine this question further, frequencies of occurrence of various sets of gage rainfall events were computed for a variety of rain gage network types. The definition of an "event" is, again, the occurrence at a gage location of an amount of rain sufficient to be useful in making comparisons with radar rainfall estimates. Because most of the subsequent calculations are based solely on radar data, we either assume that "some echo" is equivalent to "some rain" or (where indicated) require some minimum radar estimated rainfall amount. The first type of network considered involves random placement of the gages. Such a network design is not likely to be used in practice, but it provides a simple model for calculating the frequencies of gage events.

To arrive at the frequency of events for a randomly distributed rain gage network, consider the following: For a random network of n gages, the chance that the echoes in a given time interval will miss all the gages is $(1 - a_i)^n$, where $a_i$ is the fractional area coverage. For example, for three rain gages in the radar surveillance area and an echo area coverage of $a_i = 0.05$ (5%), the chance that the echoes would miss all three gages would be $(1 - 0.05)^3 = 0.86$. Expressing this idea for all possible area coverages and time intervals yields the relative frequency f with which the echo would miss all n gages:

$$f = \frac{1}{M} \sum_{i=1}^{M} (1 - a_i)^n \qquad (3)$$

where M = total number of intervals of the specified duration; $a_i$ = area coverage for the ith interval; and n = number of randomly distributed rain gages in the network. The relative frequency of occurrence of at least one gage event is then (1 - f).

Table 3 presents the resulting frequencies of occurrence for at least one gage event in a randomly distributed network of n gages. Figure 8 shows the same results for the random networks plotted with the time interval as a parameter. As expected, with increasing numbers of gages, or as the accumulation time interval increases, the frequency of occurrence of at least one gage event (some echo over a rain gage) increases. To get at least one gage event 50% of the time requires only about 8 to 16 gages for three-hour to one-hour intervals according to this computation. However, the rate of increase in the frequency of gage events diminishes for more than 20 to 30 rain gages for all time intervals of an hour or longer. (For "instantaneous" time intervals, the frequencies continually increase up to at least 60 gages.) Thus it requires at least 48 gages to be sure of having at least one event 80% of the time. The increase in the relative frequency of gage events is approximately 7% to 14% when the time interval is changed from one hour to three hours.

The same law of diminishing returns with increasing numbers of gages shows up in the results for symmetrical networks discussed in the next chapter. In a system employing real-time acquisition of rain gage data through the use of telemetering gages, it does not appear practical to install enough gages to be certain of obtaining events whenever rain is occurring within the radar surveillance umbrella. For example, according to Table 3 to obtain at least one gage event in three-fourths of all the three-hour intervals would require more than 30 gages. However, doubling the number of gages to 60 only increases the yield to about 82% of the intervals. One possible interpretation of these results is that the most cost-effective network design would involve about 20 to 30 gages per radar installation.

*TABLE 3:* Frequencies of occurrence (%) for at least one rain gage event in a randomly distributed network, for different time intervals. The "area per gage" values are based on the NCPR-1 analysis area of 38,478 $km^2$.

| No. of Gages | Area per Gage | TIME INTERVAL | | | |
|---|---|---|---|---|---|
| | | Instantaneous | 1-Hour | 2-Hour | 3-Hour |
| 3 | 12826 | 7.0 | 19.3 | 25.6 | 30.5 |
| 6 | 6413 | 12.7 | 31.2 | 39.1 | 44.9 |
| 12 | 3207 | 21.5 | 45.4 | 53.5 | 59.2 |
| 18 | 2138 | 28.0 | 53.8 | 61.3 | 66.6 |
| 21 | 1832 | 30.7 | 56.8 | 64.1 | 69.1 |
| 27 | 1425 | 35.4 | 61.6 | 68.2 | 72.9 |
| 30 | 1283 | 37.4 | 63.5 | 69.8 | 74.4 |
| 36 | 1069 | 41.0 | 66.7 | 72.4 | 76.8 |
| 42 | 916 | 44.1 | 69.2 | 74.3 | 78.7 |
| 48 | 802 | 46.8 | 71.3 | 75.9 | 80.2 |
| 54 | 713 | 49.2 | 73.0 | 77.3 | 81.5 |
| 60 | 641 | 51.4 | 75.4 | 78.4 | 82.5 |

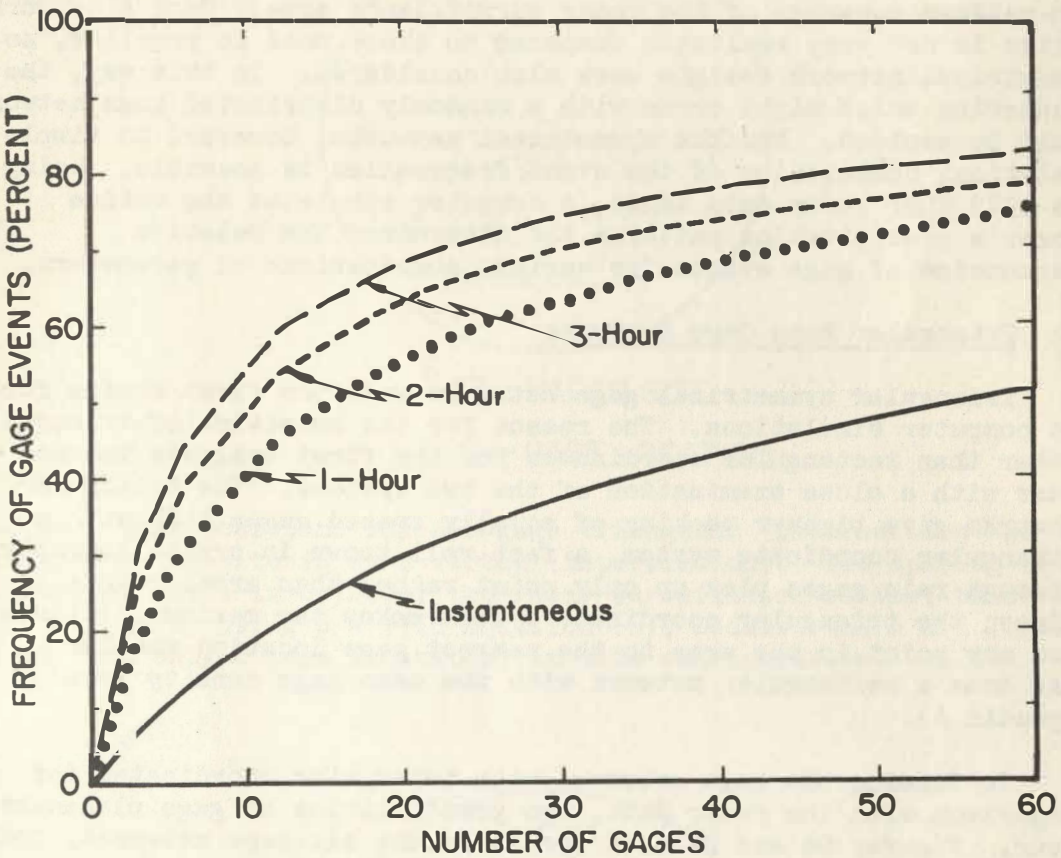


*Fig. 8.* Frequency of at least one gage event vs. the number of rain gages in a randomly distributed gage network, for various data accumulation time intervals. For these curves, any radar echo constitutes an event.

## 5. FREQUENCIES OF GAGE EVENTS FOR SYMMETRICAL GAGE NETWORKS

Placing rain gages in a randomly distributed fashion would provide non-uniform coverage of the radar surveillance area. Such a network design is not very realistic compared to those used in practice, so symmetrical network designs were also considered. In this way, the clustering which might occur with a randomly distributed gage network would be avoided. For the symmetrical networks, however, no simple analytical computation of the event frequencies is possible. Using the 1972 NDPP radar data tapes, a computer simulated the entire summer's precipitation patterns and determined the relative frequencies of gage events for various combinations of parameters.

### 5.1 Triangular Rain Gage Networks

Triangular symmetrical gage networks were the first choice for the computer simulations. The reason for the selection of triangular rather than rectangular coordinates for the first analysis becomes clear with a close examination of the two systems. The triangular networks give tighter packing of equally spaced gages than with a rectangular coordinate system, a fact well known in crystallography. Although rain gages pick up only point rather than areal rainfall values, the triangular coordinate system makes the maximum distance from any point in the area to the nearest gage location smaller than does a rectangular network with the same gage density (see Appendix A).

In forming the gage networks with triangular coordinates for comparison with the radar data, two possibilities of gage placement occur. Figures 9a and 9b show two different six-gage networks, both with triangular symmetry. Figure 9a shows the gage locations when the radar site is placed at an intersection point in the triangular grid. This type of arrangement is hereafter referred to as an "intersection" gage network. Figure 9b shows the gage locations produced when the radar site is placed at the center of one of the equilateral triangles in the grid. This type of configuration will be referred to as a "center" gage network. Thus the adjective used denotes the location of the radar site in the coordinate grid.

Both the center and intersection triangular networks have the desired symmetry, but there are some differences with small numbers of gages. The intersection-type networks place all the gages out towards the periphery of the radar surveillance area. This seemingly would reduce the coverage of echoes occurring close to the radar site where the radar is somewhat more sensitive. The center-type networks have some gages nearer the radar site, but provide rather sparse coverage at greater distances. The significance of the differences diminishes, and the uniformity of coverage improves, as the numbers of gages in the networks increase.

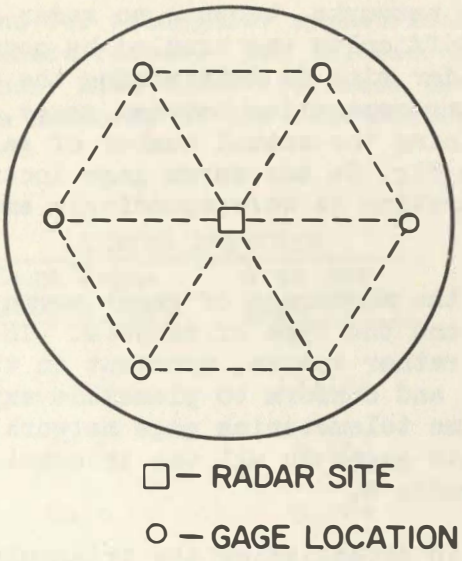


*Fig. 9a.* Gage positions for a 6-gage triangular "intersection" network where the radar site is at a vertex (intersection). The spacing between neighboring gages is 0.720 of the radar surveillance radius; this value was obtained by using n = 7 in Equation (6), because there are 7 grid points (but only 6 gage locations) in this configuration.

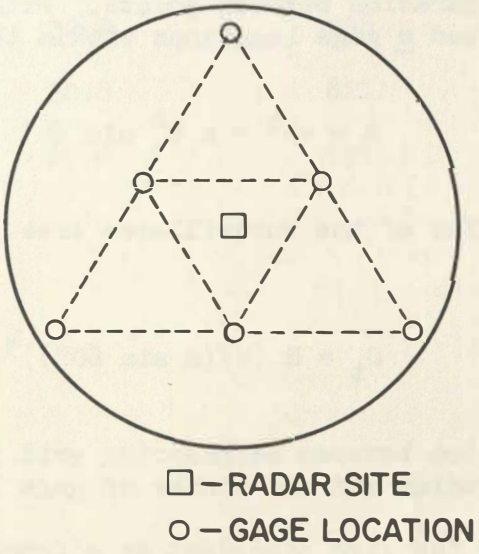


*Fig. 9b.* Gage positions for a 6-gage triangular "center" network where the radar site is in the center of a triangle. The spacing between neighboring gages is 0.778 of the radar surveillance radius, as found by using n = 6 in Equation (6).

There is also a problem with the grid location at the radar site in the intersection networks, because no radar data are available for that point. This difficulty was handled by counting the "pseudo-gage location" at the radar site in determining the number of gage locations and the corresponding separation between gages, but then omitting that location in determining the actual number of gages in the network. Thus the network in Fig. 9a has seven gage locations (but only six gages) and the separation is correspondingly smaller than that in Fig. 9b.

Table 4 shows the numbers $\underline{n}$ of gages corresponding to each individual network and the type of network. The gage densities for these networks are rather sparse, somewhat in the area that Wilson (1970) worked with, and conform to plausible expectations for an operational real-time telemetering gage network. To see the specific placement of the rain gages in all the triangular networks, the reader is referred to Appendix B.

The next step in establishing the triangular gage networks for the computer simulation was determining the separation between neighboring grid points (or gage locations). Each gage in a triangular grid represents a unit area $\underline{a}$ consisting of a parallelogram with equal sides and 60°/120° junctions:

$$a = S_t^2 \sin 60° \tag{4}$$

where $S_t$ is the separation between points. With A as the overall radar surveillance area and $\underline{n}$ gage locations within that area:

$$A = \pi R^2 = n\, S_t^2 \sin 60° \tag{5}$$

where R is the radius of the surveillance area. This then yields the expression

$$S_t = R\,[\pi/(n \sin 60°)]^{\frac{1}{2}} \tag{6}$$

giving the separation between neighboring grid points as a function of the surveillance radius and the number of gage locations.

By expressing the gage placement as a function of the radar surveillance radius, the frequencies of gage events shown in the next section can be applied to any surveillance area. This statement relies

*TABLE 4:* Specifications for triangular symmetrical rain gage networks in a 112-km radar surveillance radius. The intersection networks include a "pseudo" gage at the radar site which decreases the area per gage when compared to center gage networks of the same number of gages.

| No. of Gages | Type | CENTER NETWORKS | | INTERSECTION NETWORKS | |
|---|---|---|---|---|---|
| | | Gage Separation (km) | Area per gage ($km^2$) | Gage Separation (km) | Area per gage ($km^2$) |
| 3 | C | 123.2 | 13,136 | | |
| 6 | C,I | 87.1 | 6,568 | 80.6 | 5,630 |
| 12 | C,I | 61.6 | 3,284 | 59.2 | 3,031 |
| 18 | C,I | 50.3 | 2,189 | 48.9 | 2,074 |
| 21 | C | 46.5 | 1,877 | | |
| 27 | C | 41.1 | 1,460 | | |
| 30 | C,I | 38.9 | 1,314 | 38.3 | 1,271 |
| 36 | C,I | 35.6 | 1,095 | 35.1 | 1,065 |
| 42 | C,I | 32.9 | 938 | 32.5 | 916 |
| 48 | C | 30.8 | 821 | | |
| 54 | C,I | 29.0 | 730 | 28.8 | 717 |
| 60 | I | | | 27.3 | 646 |

C - "Center" network

I - "Intersection" network

upon the assumptions that the frequency distributions of echo area coverage (Fig. 4) will remain constant for any surveillance area and, for use in other geographic locations, the results of the analysis are directly transferable. The subject of transferability of results is discussed in Chapter 6.

With the above formula for gage separation and ordinary trigonometry, the triangular grid coordinates can be transformed into the range-azimuth (r-θ) system used on radar PPI displays and in the recorded NCPR-1 data. After transforming the various gage networks into the range-azimuth system, each gage location was associated with a specific radar range-azimuth bin for the computer simulation.

## 5.2 Gage Event Frequencies for Triangular Networks

The relative frequencies of gage events for each gage network were obtained by simulating a summer's precipitation over the various networks. This was accomplished by passing the entire summer's tape recorded radar data over each network on a computer. For this analysis, only situations with some echo present somewhere in the surveillance area were used, so that the relative frequencies obtained are in terms of those time periods with some echo present. Graphs were generated for different time intervals and criteria for whether an event was counted. For reasons of simplicity, the graphs presented in this section concentrate on the three-hour time intervals except where a special point is to be made. Similarly, the graphs selected also concentrate on the center networks. Other graphs generated for various time intervals and network designs not shown in this section can be found in Appendix C.

### 5.2.1 Comparison of center, intersection, and random networks

A comparison of the relative frequencies of gage events for symmetrical networks with those calculated for randomly distributed gage networks in Chapter 4 is shown in Fig. 10. In general, the results are quite similar, especially for the larger numbers of gages. The center networks show higher event frequencies for small numbers of gages. A possible explanation of this difference lies in the discussion of Figs. 9a and 9b in the previous section. In the smaller gage networks, more rainfall occurrences (as indicated by radar echoes) near the radar site were presumably undetected by the intersection networks, yielding lower relative frequencies. The center networks, which place more gages near the radar site, achieved higher relative frequencies of gage events than the other two configurations, but the differences decrease as the number of gages increases.

One inference that can be drawn from the similarity of the results for the random and symmetrical networks is that for the sparse networks

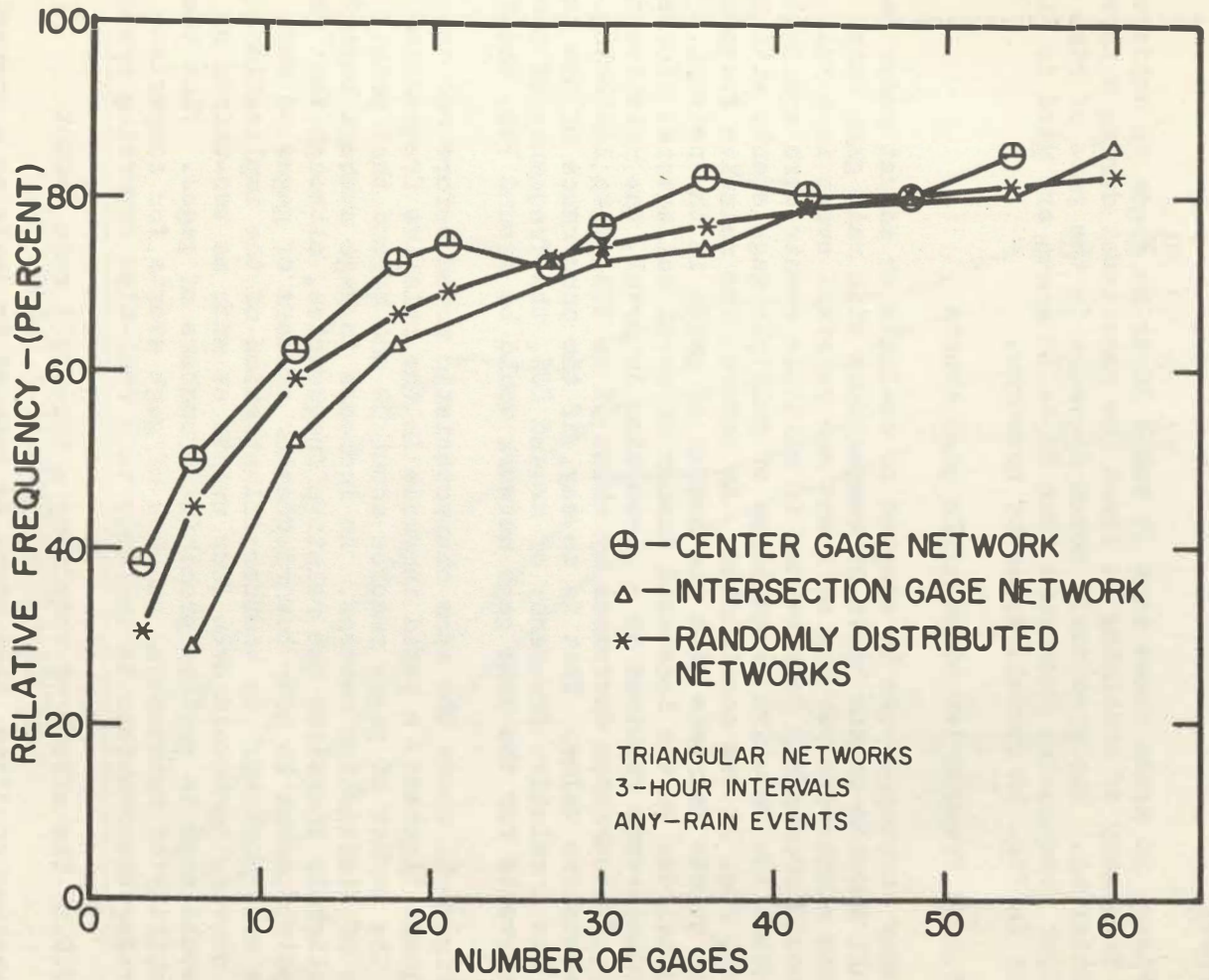


*Fig. 10.* Comparison of event frequencies for triangular (center and intersection) gage networks to those for a randomly distributed network. The relative frequency indicated is that of at least one rain gage event (of any rainfall amount) occurring within a 3-hour time interval.

considered here the rainfall occurrences at different gage locations are independent events. Were that not the case, the specific gage placement would have greater influence on the event frequencies. Because the observed differences among the network types are not large, we use the center-network results for illustrative purposes henceforth.

Figure 10 again shows that it takes 30 or so gages to achieve a 75% frequency of obtaining at least one gage event during a three-hour interval. The previously noted decrease in the rate of rise of the event frequencies when more than 20 to 30 gages are used is also evident in Fig. 10 for all types of networks.

5.2.2 Frequencies of multiple gage events

Many strategies can be adopted to evaluate or adjust radar estimated rainfall amounts on the basis of comparisons with rain gage data. All of these strategies require at least one rainfall event in a rain gage. Most would presumably work better if multiple events were available. To present the relative frequencies of multiple gage events within a network, Fig. 11 was constructed. As before, the relative frequencies of gage events increase with the number of gages in the network. This is logical due to the increased number of event collectors. For each additional event required in a given time interval, the relative frequency of occurrence decreases by about 5% to 20%, with 10% being a representative value. That is to say, if the occurrence of one gage event has a relative frequency of around 80%, the frequency of occurrence of two events for the same gage network would be around 70%, and so on.

Figure 11 shows the same characteristic noted before and in subsequent figures: a rapid increase in the relative frequencies until the number of gages reaches about 30 and beyond that point, a region of diminishing returns. An increase in gage numbers beyond 30 only slightly increases the relative frequencies, although the "saturation point" seems to move toward greater numbers of gages as more events are required. As another illustration of the implications of these curves, to obtain even four events as much as two-thirds of the time would seem to require prohibitive numbers of gages. Thus the availability of substantial numbers of gage events for comparison with radar observations is unlikely in a real-time reporting system.

5.2.3 The effect of requiring a threshold rain amount

Another condition that might be imposed in devising a comparison strategy is to require some minimum rainfall amount in the gage before counting the precipitation as a gage event. Application of this type of criterion has been tested in Fig. 12. The rainfall accumulations at the gage locations were computed by time integration of the rainfall rates determined from Equation (2). As to be expected, when the

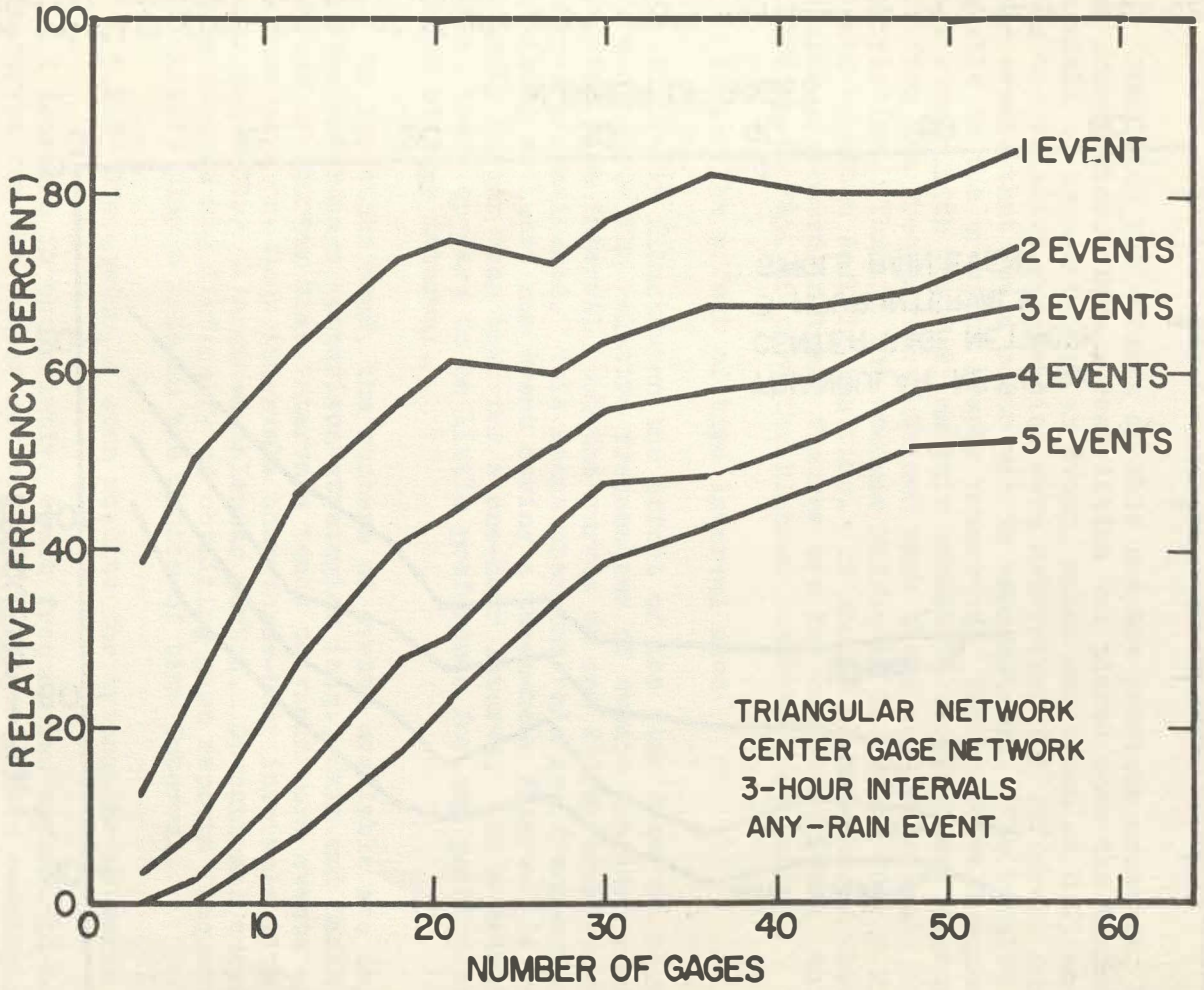


*Fig. 11.* Relative frequencies of multiple rain gage events (of any rainfall amount) in triangular center networks, for 3-hour time intervals.

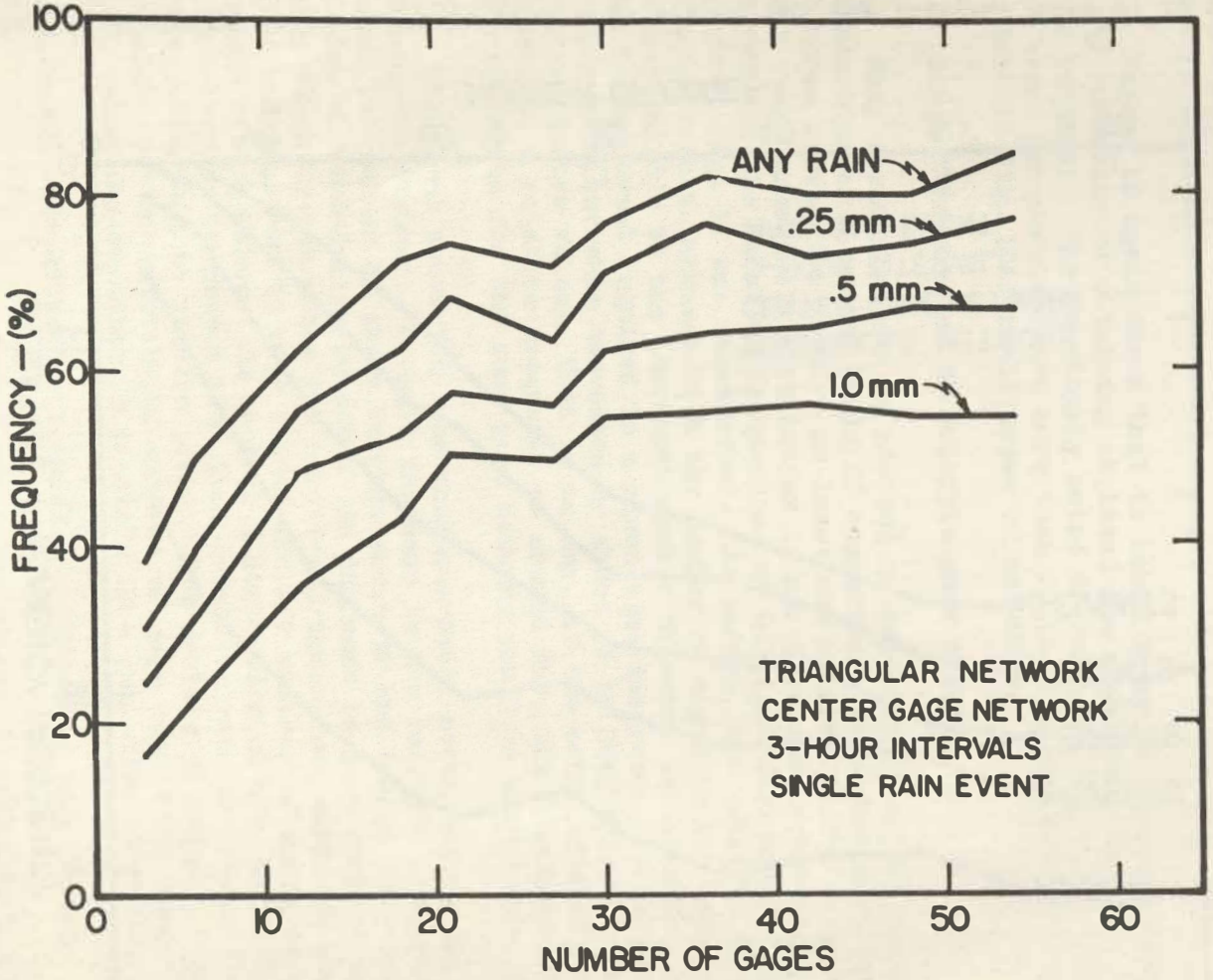


*Fig. 12.* The relative frequencies of single gage events required to be greater than or equal to specified rainfall amounts, for triangular center networks and 3-hour time intervals.

acceptable threshold value of rainfall amount increases, the relative frequencies of usable gage events decrease. A requirement to have at least 1.0 mm (0.04 inch) in the gage would mean that even single events would be available in only slightly more than half the instances even with a network of more than 30 gages. The other characteristics of the graphs described earlier remain.

Combining the effects of this and the previous criteria, Fig. 13 was constructed. Here a restriction was placed upon the minimum gage rainfall to be counted as an event, which was taken as 0.25 mm (0.01 in). Then the relative frequencies were determined for different numbers of gage events that would occur within each network. The results are comparable to the previous graphs presented. The relative frequencies of gage events with the 0.25 mm rain threshold were reduced approximately 10% from the frequencies obtained when there was no rainfall threshold restriction. Thus it now becomes difficult to obtain four 0.25 mm events as often as half the time. It should be remembered that the results presented in these figures are for center networks, which according to Fig. 10 give the highest relative frequencies.

### 5.2.4 The effect of time interval used

Figure 14 illustrates the effect of the time interval chosen for the analysis. The relative frequencies of events increase somewhat with the time interval, but the curves do not differ greatly among the intervals considered. This means that the relative frequency of obtaining at least one event during a three-hour interval is only slightly larger than that for a one-hour interval. On a relative basis, there appears to be little preference for any particular choice of time interval.

On the other hand, the numbers of events available are important in some radar-gage comparison strategies (e.g., Cain and Smith, 1977). The use of shorter time intervals tends to yield more events simply because more one-hour intervals than three-hour intervals with some radar echo occur in a given calendar period. Operational considerations such as the difficulty of obtaining gage reports frequently will likely play a role in the choice of time interval.

### 5.2.5 Discussion of some results for triangular networks

A decrease in the relative event frequencies appears in many of the curves for the center networks at 27 gages. This seemingly is an odd circumstance; given additional radar data for the simulation, it presumably would not have happened. Possibly the 1972 precipitation echoes tended to fall between the gage sites for the 27-gage center pattern so that an inordinate number of precipitation events somehow missed the network.

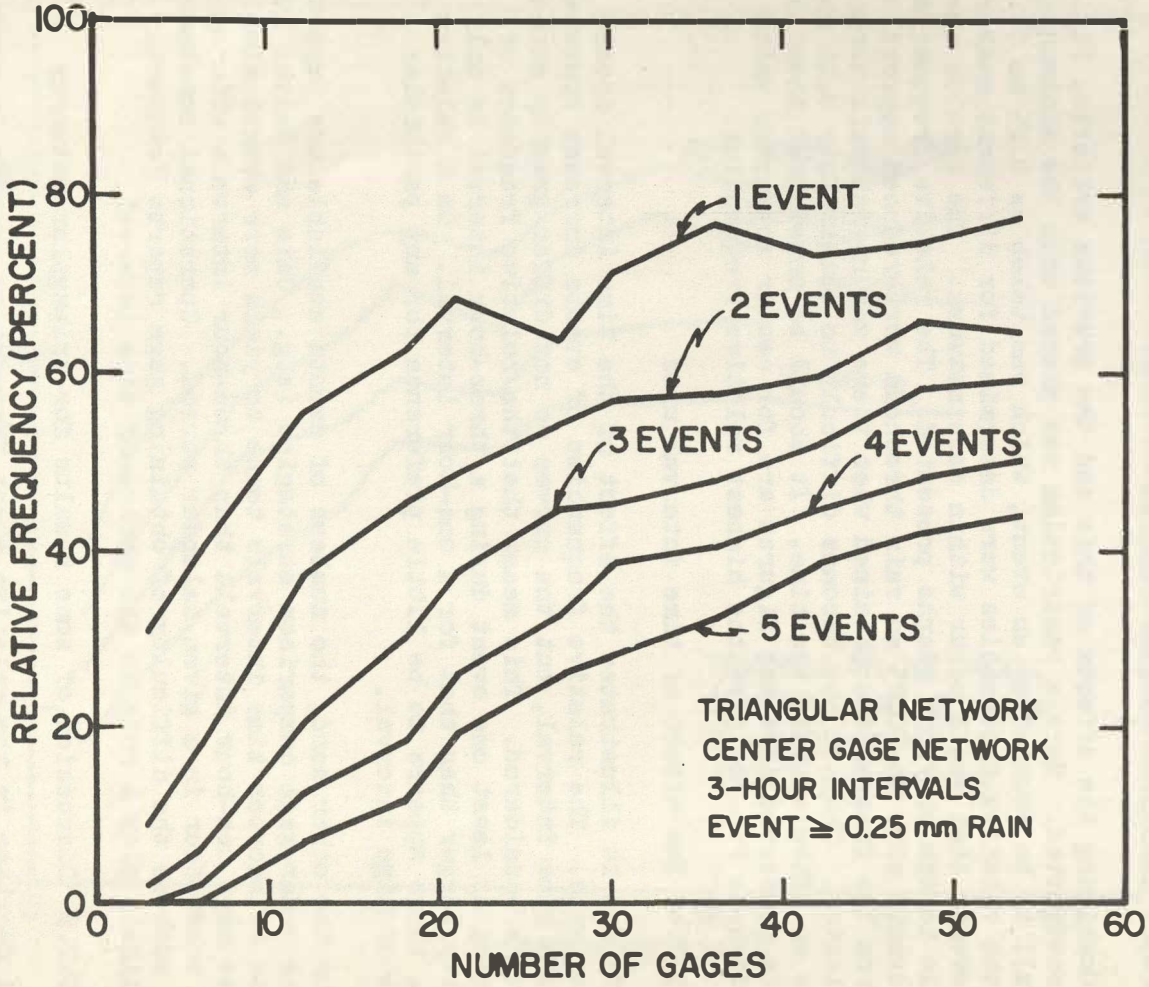


*Fig. 13.* Relative frequencies of multiple rain gage events, with each event having a rainfall amount ≥0.25 mm. Results shown are for triangular center networks and 3-hour data collection time intervals.

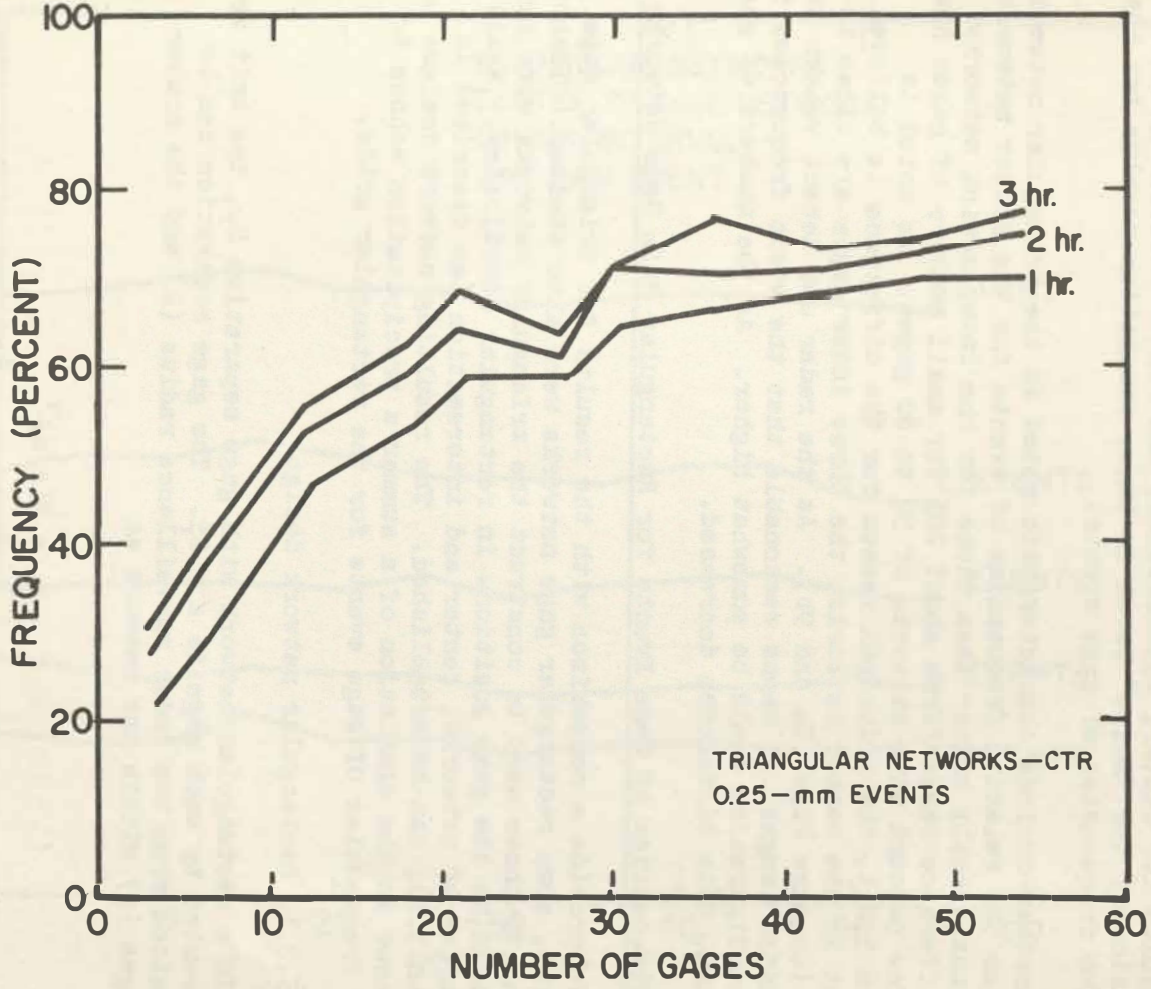


*Fig. 14.* Relative frequencies of obtaining at least one gage event of 0.25 mm or more, as a function of the number of gages with time interval as a parameter. The curves are for triangular center networks.

To see if this was the case, that the gage pattern was rotated around the radar site (retaining its triangular symmetry) by increments of 5°. Figure 15 shows the results of this simulation. The variations of the relative frequencies through this rotation were not significant and, hence, show that the specific rain gage locations did not greatly affect the frequencies generated. Figure 15 plus the differences among the results for center, intersection, and random networks give some indication of the "noise" level in these simulation results for the relative frequencies of gage events.

Another curious characteristic noted in the triangular networks was that the relative frequencies of events for the center networks were consistently higher than those for the intersection networks. The difference ranged from about 20% for small numbers of gages down to a few percent with networks of 50 to 60 gages. As noted in Section 5.2.1, the principal reason for the difference is believed to be that in the center networks, the three inner gages are close to the radar (compare Figs. 9a and 9b). As the radar can detect weaker echoes at shorter ranges, it seems reasonable that the event frequencies for this configuration would be somewhat higher. As the numbers of gages increase, this difference decreased.

## 5.3 Frequencies of Gage Events for Rectangular Rain Gage Networks

To provide a comparison with the results for triangular gage networks, some rectangular gage networks were also studied. Techniques similar to those used to construct the triangular networks were employed to determine the gage positions in rectangular coordinates. Again two categories of networks, center and intersection (as described in Section 5.1), can be established. The resulting network designs were then used in the simulation of a summer's precipitation echoes to yield frequencies of gage events for the rectangular grids.

### 5.3.1 Rectangular network design

In a rectangular network with gage separation $S_r$, the unit area represented by each gage is $a = S_r^2$. The gage separation can be determined from the radar surveillance radius (R) and the number of gages (n) within the network as

$$S_r = R(\pi/n)^{\frac{1}{2}} \qquad (7)$$

Thus for a given number n of gages in the network, comparison of (7) with (6) shows that the separation between gage locations in a rectangular grid will be smaller than that for a triangular grid by a

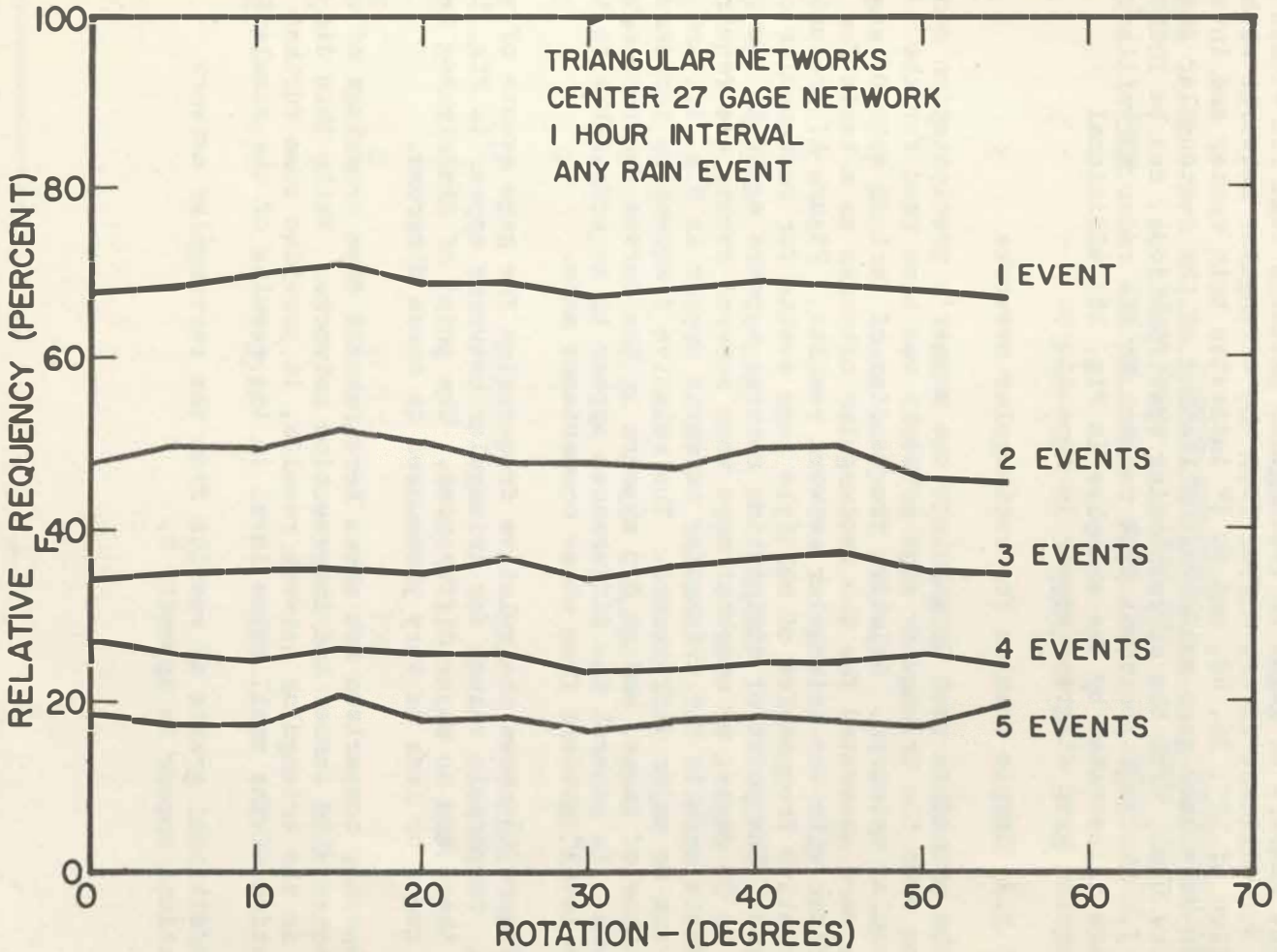


*Fig. 15.* The relative frequencies of multiple gage events when a triangular center 27-gage pattern is rotated around the radar site by 5° increments. The number of gage events within a 1-hour time interval is the parameter; any amount of rainfall is considered an event. No marked variations relatable to specific gage placement are evident.

factor 0.93. As pointed out in Appendix A, however, the triangular geometry results in a smaller maximum distance from any point to the nearest gage location.

The numbers of gages in rectangular patterns that fit within the radar surveillance circle differ from the triangular networks with the exception of 12*, 36, 48, and 60 (* indicates both center and intersection versions) gage networks. A listing of the rectangular gage networks used, with the corresponding specifications, can be found in Table 5. The gage positions with respect to the radar surveillance area are illustrated by the examples in Fig. 16; additional rectangular grid diagrams appear in Appendix D.

5.3.2 Sample results for rectangular networks

The procedure used to simulate the summer's precipitation echoes passing over the triangular gage networks was also used for the rectangular networks. Relative frequencies of various sets of gage events were generated for the rectangular networks as a basis for comparison with the triangular network results. Figure 17 presents the relative frequencies of multiple gage events for rectangular center networks. The point of diminishing returns appears again in the range of 20 to 30 gages, or somewhat more when several events are required. Comparable results for triangular networks appear in Fig. 11, and there are no major differences. The relative frequencies increase with the number of gages, and no dip appears in the curves for rectangular networks. In general the differences appear to be comparable to the "noise level" evident from other comparisons made.

Figure 18 shows the relative frequencies for gage events of various sizes. Comparable values for triangular networks appear in Fig. 12, and again there are no major differences. The point of diminishing returns at 30 gages or less is very pronounced in these diagrams.

Another comparison not shown here reveals some crossings of curves for rectangular center and intersection networks. While this did not occur in the triangular network results, it provides some further indication of the small noise level in the results of the simulations.

Additional graphs of results from the rectangular network simulations appear in Appendix D.

*TABLE 5:* Specifications for rectangular symmetrical rain gage networks, in a 112-km radar surveillance radius.

| No. of Gages | Type | CENTER NETWORKS | | INTERSECTION NETWORKS | |
|---|---|---|---|---|---|
| | | Gage Separation (km) | Area per gage ($km^2$) | Gage Separation (km) | Area per gage ($km^2$) |
| 4 | C,I | 99.3 | 9,852 | 88.8 | 7,882 |
| 8 | I | | | 66.2 | 4,379 |
| 12 | C,I | 57.3 | 3,284 | 55.1 | 3,031 |
| 16 | C | 49.6 | 2,463 | | |
| 20 | I | | | 43.3 | 1,877 |
| 24 | C,I | 40.5 | 1,642 | 39.7 | 1,576 |
| 28 | I | | | 36.9 | 1,359 |
| 32 | C | 35.1 | 1,232 | | |
| 36 | I | | | 32.6 | 1,065 |
| 44 | C,I | 29.9 | 896 | 29.6 | 876 |
| 48 | I | | | 28.4 | 804 |
| 52 | C | 27.5 | 758 | | |
| 56 | I | | | 26.3 | 691 |
| 60 | C,I | 25.6 | 657 | 25.4 | 646 |

C - "Center" network

I - "Intersection" network

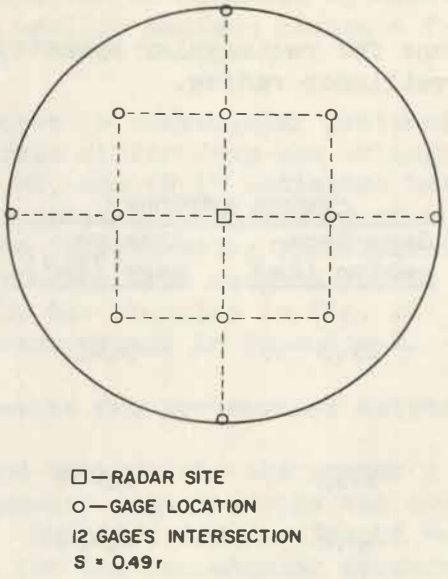


*Fig. 16a.* Gage positions for a 12-gage rectangular "intersection" network. The distance between gages (S) is 0.492 of the radar surveillance radius; this value was obtained by taking n = 13 in Equation (7), counting the 13 gage locations (but only 12 gages) in this configuration.

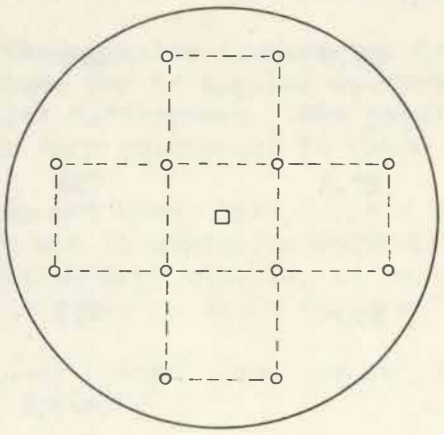


*Fig. 16b.* Gage positions for a 12-gage rectangular "center" network. The separation between gages (S) is 0.512 of the radar surveillance radius, as found by using n = 6 in Equation (7).

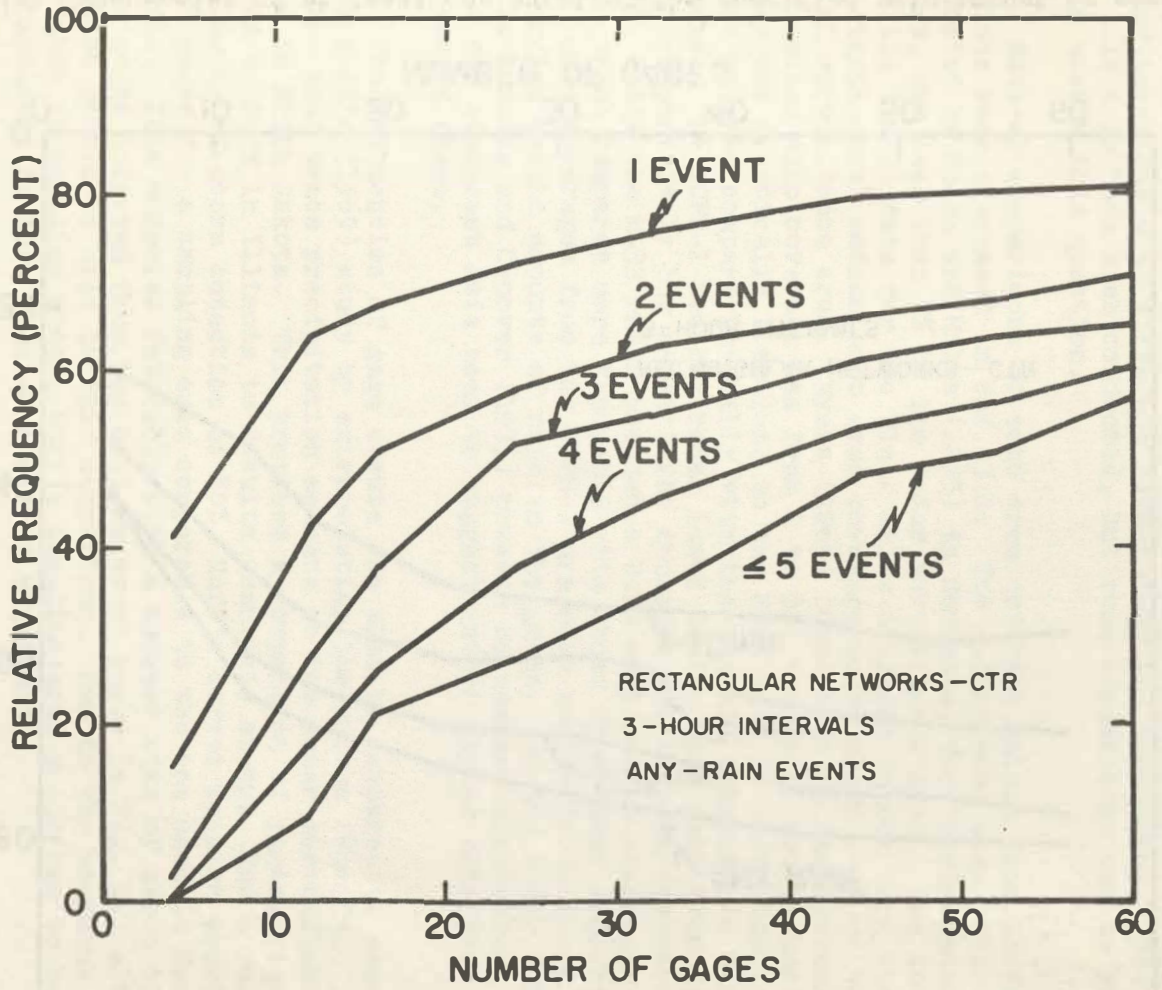


*Fig. 17.* Relative frequencies of multiple rain gage events (of any rainfall amount) in rectangular center networks, for 3-hour time intervals.

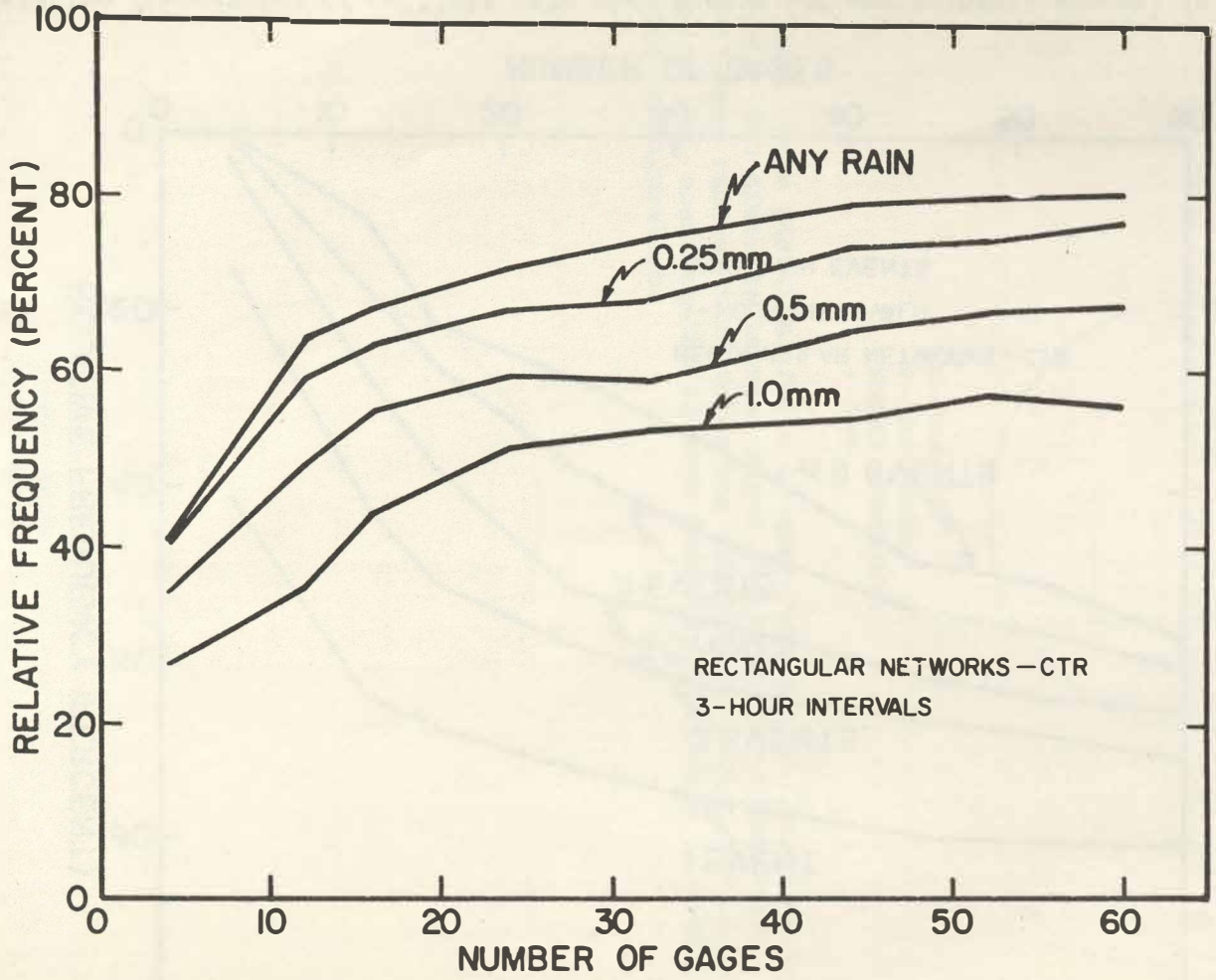


*Fig. 18.* Relative frequencies of at least one event of the specified rain amount or more, for rectangular center networks and 3-hour time intervals.

# 6. TRANSFERABILITY OF RESULTS

The radar data used for this study were collected in a semi-arid region with mean annual precipitation of less than 20 inches (50 cm). It is reasonable to ask whether the results obtained can be applied to other locations with different climatology and topography. Few studies of this type have been conducted, but some comparisons can be made to help answer this question.

Several comparisons of echo area coverage values from different regions were discussed in Sec. 3.2. The median echo area coverage reported by Soane and Miles (1955) in Rhodesia, for "instantaneous" views, was less than 3% of the radar surveillance area. The Kuo and Orville (1973) data for the Black Hills of South Dakota show the "instantaneous" median echo area coverage to be about 2.5% of the total surveillance area. Myers (1964) found that in Pennsylvania the median echo coverage was from 2 to 3%; the radar system used by Myers was practically identical to the M-33 used in North Dakota. These results compare favorably with the results obtained in North Dakota. The NCPR-1 weather radar (used as the main data source) with comparatively low sensitivity showed a median echo coverage of 1.1%, while the M-33 radar yielded a 2.5% median echo coverage. The M-33 value compares more favorably with those from other regions, but the lower coverages from the NCPR-1 are more realistic in terms of inferring usable amounts of rain in the gages. On the other hand, while Bunting and Conover (1971) present no summary statistics, their data for southeast Asia seem to suggest rather higher echo area coverages there.

The frequencies of gage events can also be compared to some results from Huff's (1969) study by extrapolating the curves from Fig. 1 for summer mean trace precipitation amounts to the radar surveillance area used in North Dakota. This provides a comparison of gaging requirements found by Huff in Illinois to results from this study. For a relative frequency of storm detection of 80%, Huff's curves require about 70 rain gages for a sampling area comparable to the one used in North Dakota. This compares favorably with a network size of about 60 or more gages inferred from the 0.25 mm event curve in Fig. 12, although caution should be used in this comparison. Due to the enormous differences in sampling areas, Huff's sampling area scale had to be extrapolated by more than an order of magnitude.

These limited comparisons suggest that the results presented herein may provide useful guidelines for other locations with continental climates. This applies particularly to the gage event frequencies, which are determined primarily by the echo area coverage statistics. It may be that differences in annual rainfall amounts among various locations are due mainly to a combination of more hours with rain, and

higher rainfall rates during the rainy periods, rather than to differences in the fractional echo area coverage. However, it is clear that this inference should be tested by conducting similar studies for other geographic locations.

Another logical question is whether the various results presented herein are independent of the size of the radar surveillance area. No definitive answer can be given, because only one area was used in the analyses. For the present we hypothesize that this area is large enough to provide representative statistics. If that were true, application of the results to an enlarged area of, say, 200 km radius would still require the same numbers of gages to achieve the same event frequencies. Obviously this hypothesis also needs to be verified by further investigations.

## 7. CONCLUSIONS AND DISCUSSION

The general answer to the question raised in Section 1.1 is that for any small number of gages such as seem reasonable for a real-time reporting network, one should expect usually no more than about five gage events (reports) within the time intervals that are likely to be of operational interest. For example, with a 30-gage network even single events would be available for less than 80% of the three-hour intervals when echoes appear in the radar surveillance area (Fig. 10). As many as four events would be available in less than half of the intervals (Fig. 11). Consequently, some techniques for comparing radar and rain gage data such as that proposed by Brandes (1975) do not appear to be feasible for use in real-time operational systems for radar measurement of rainfall. The numbers of gage events (data points) will be too small to permit effective use of the techniques in real time.

A prominent characteristic found throughout the simulations was that for more than about 20 to 30 gages in a network, the rate of increase of relative event frequencies diminishes sharply. Figure 10 illustrates this property of diminishing returns, as do many of the other figures presented. In Fig. 10, the relative frequencies of events increase with the number of gages up to about 75% with 30 gages. A further increase to more than 50 gages brings the relative frequencies up to only slightly above 80%. The relatively small increases in event frequencies for networks of more than 20 to 30 gages suggest that this size may be the most effectual to employ in operational networks. Perhaps a network of about 25 gages can be regarded as a reasonable compromise.

The supposition is that the study area was large enough to yield representative echo coverage statistics, so that the required numbers of gages will not depend upon the specific value of the surveillance radius. Comparing rectangular versus triangular network grids of various configurations but with the same numbers of gages showed no consistent differences. The inference here is that the results are not strongly dependent upon specific gage placement.

There is a slight time-dependence for the numbers and the rainfall amounts of gage events for any given network. Taking the triangular center networks as an example, the relative event frequencies increase about 5 to 8% when going from one-hour intervals to two- or three-hour intervals. This increase is small enough that the reporting interval does not seem to be a major factor in network design based on relative event frequencies. However, there are more one-hour than three-hour intervals in a given calendar period, so the absolute numbers of events should increase if shorter time intervals are used.

The North Dakota area in which the radar data were collected is semi-arid, with mean annual precipitation of less than 20 inches. Corresponding statistics for areas with greater rainfall may show higher event frequencies, although it may well turn out that the major differences will be in greater numbers of hours with echoes, within which the statistics differ little from those reported here. The few comparisons which could be made with data from other locations suggest that the area coverage and event frequency statistics are likely to be much the same. However, similar analyses of data from such areas would be useful in generalizing the statistics presented here to provide broader guidelines for the design of gage networks to support operational radar rainfall measurements.

## ACKNOWLEDGMENTS

**The computer simulations were accomplished by Mr. Douglas E. Cain using the Computer Center of South Dakota School of Mines and Technology. The manuscript was typed by Mrs. Joie L. Robinson, and figures within the text were drafted by Mr. Melvin J. Flannagan.**

## REFERENCES

Brandes, E. A., 1975: Optimizing rainfall estimates with the aid of radar. J. Appl. Meteor., 14, 1339-1345.

Bunting, J. T., and J. H. Conover, 1971: On the accuracy of a precipitation coverage index computed from radar reports. J. Appl. Meteor., 10, 224-227.

Cain, D. E., and P. L. Smith, Jr., 1977: A sequential analysis strategy for adjusting radar rainfall estimates on the basis of rain gage data in real time. Preprints 2nd Conf. Hydrometeorology, Toronto, Amer. Meteor. Soc., 280-285.

Dennis, A. S., and F. G. Fernald, 1963: Frequency distributions of shower sizes. J. Appl. Meteor., 2, 767-769.

_____, J. R. Miller, Jr., E. I. Boyd, and D. E. Cain, 1975: Effects of cloud seeding on summertime precipitation in North Dakota. Report 75-1, Institute of Atmospheric Sciences, South Dakota School of Mines and Technology, Rapid City, South Dakota. 97 pp.

Huff, F. A., 1967: The adjustment of radar estimates of storm mean rainfall with rain gage data. J. Appl. Meteor., 6, 52-56.

_____, 1969: Precipitation detection by fixed sampling densities. J. Appl. Meteor., 8, 834-837.

_____, 1970: Sampling errors in measurement of mean precipitation. J. Appl. Meteor., 9, 35-44.

Kuo, J. T., and H. D. Orville, 1973: A radar climatology of summertime convective clouds in the Black Hills. J. Appl. Meteor., 12, 359-368.

Miller, J. R., Jr., and D. E. Cain, 1973: The North Dakota Pilot Project evaluation of data - 1972. Report 73-3, Institute of Atmospheric Sciences, South Dakota School of Mines and Technology, Rapid City, South Dakota. 50 pp.

Myers, J. N., 1964: Preliminary radar climatology of central Pennsylvania. J. Appl. Meteor., 3, 421-429.

Smith, P. L., Jr., D. E. Cain, A. S. Dennis, and J. R. Miller, Jr., 1975: Determination of R-Z relationships for weather radar using computer optimization techniques. Report 75-3, Institute of Atmospheric Sciences, South Dakota School of Mines and Technology, Rapid City, South Dakota. 89 pp.

Soane, C. M., and V. G. Miles, 1955: On the space and time distributions of showers in a tropical region. Quart. J. Roy. Meteor. Soc., 81, 440-448.

Wilson, J. W., 1970: Integration of radar and rain gage data for improved rainfall measurement. J. Appl. Meteor., 9, 489-497.

Woodley, W. L., A. R. Olsen, A. Herndon, and V. Wiggert, 1974: Optimizing the measurement of convective rainfall in Florida. NOAA Tech. Memo ERL WMPO-18, Boulder, Colorado. 99 pp.

_____, _____, _____, and _____, 1975: Comparison of gage and radar methods of convective rain measurement. J. Appl. Meteor., 14, 909-928.

(This page intentionally left blank.)

# APPENDIX A

## The Advantage of a Triangular Network Grid

The use of a triangular grid instead of a rectangular one for laying out a rain gage network reduces the maximum distance from any point in the area involved to the nearest gage location. To demonstrate this, consider a large area A in which the number of gages n (also large) is specified. The following table compares rectangular and triangular grids.

| | Triangular Grid | Rectangular Grid |
|---|---|---|
| Unit area (area per gage) ($a = A/n$) | $a = S_t^2 \sin 60°$ | $a = S_r^2$ |
| Gage separation | $S_t = \sqrt{\frac{A}{n \sin 60°}}$ | $S_r = \sqrt{\frac{A}{n}}$ |
| Greatest distance from any point to a gage | $d_t = \frac{S_t}{2 \sin 60°}$ | $d_r = \frac{S_r}{\sqrt{2}}$ |
| | $= \sqrt{\frac{A}{2n}} \times \sqrt{\frac{1}{2(\sin 60°)^3}}$ | $= \sqrt{\frac{A}{2n}}$ |
| | $= 0.877 \sqrt{\frac{A}{2n}}$ | |

Thus the greatest distance from any point to a gage location in a triangular grid is only 87.7% of that for a rectangular network of the same gage density.

(This page intentionally left blank.)

# APPENDIX B

## Triangular Network Designs

The following figures show the positioning of rain gages in triangular networks with specified numbers of gages within a circle. The spacing ($S_t$) between gage locations is expressed as a function of the radar surveillance radius. The networks may be classified into two categories, the first one containing networks with the radar site in the center of one of the triangular lattice elements (center networks); and the second one, those where the radar site is at an intersection in the lattice (intersection networks). The diagrams are paired (center network above, intersection network below) for networks in each category containing the same numbers of gages. The gage pattern numbers are for internal reference to the way some of the computer simulation results are catalogued.

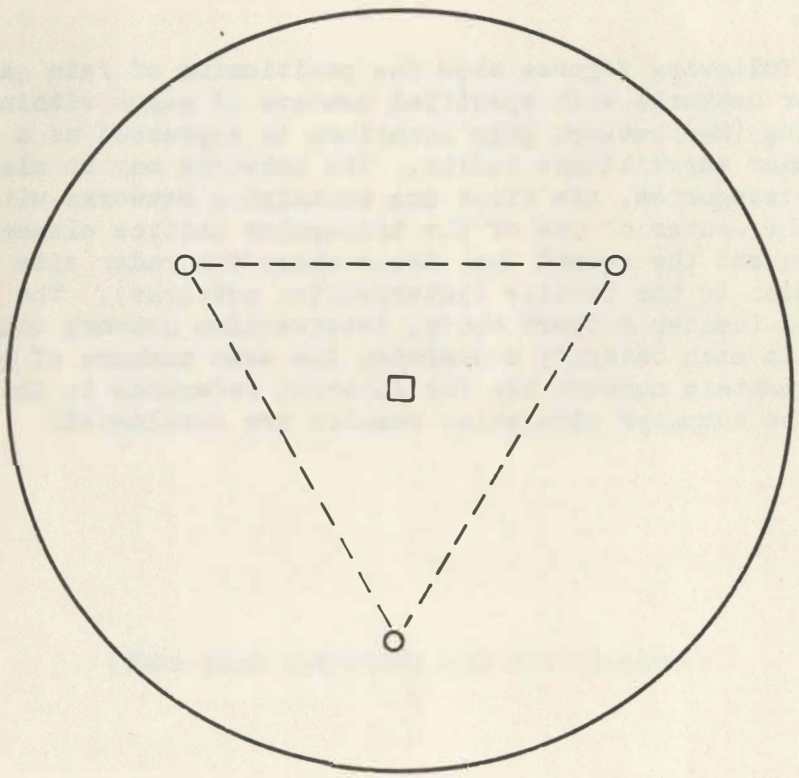

□ — RADAR SITE

○ — GAGE LOCATION

3 GAGES

S = 1.10 r

(Gage Pattern No. 9)

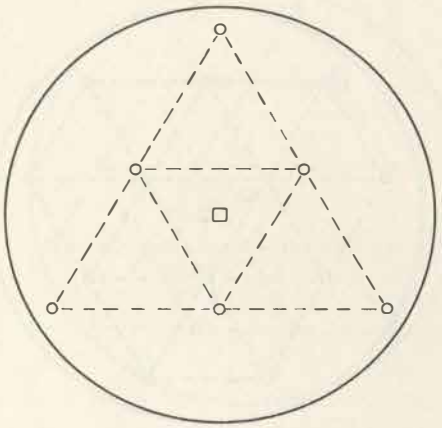

□—RADAR SITE
○—GAGE LOCATION
6 GAGES
S = 0.78 r

(Gage Pattern No. 10)

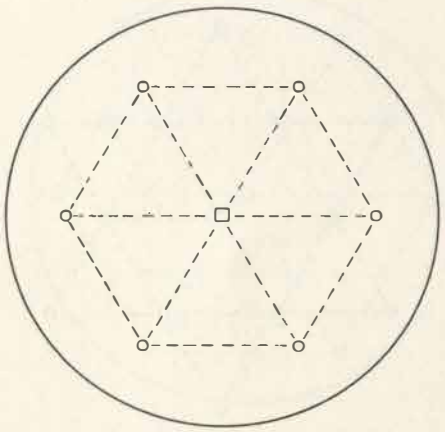

□—RADAR SITE
○—GAGE LOCATION
6 GAGES
S = 0.72 r

(Gage Pattern No. 1)

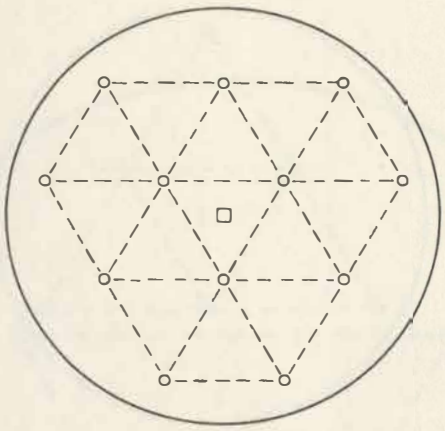

□ — RADAR SITE
o — GAGE LOCATION
12 GAGES
S = 0.55 r

(Gage Pattern No. 11)

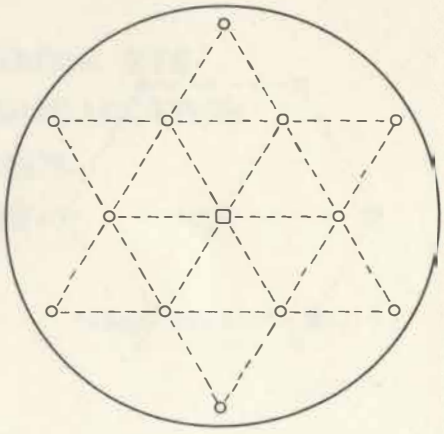

□ — RADAR SITE
o — GAGE LOCATION
12 GAGES
S = 0.53 r

(Gage Pattern No. 2)

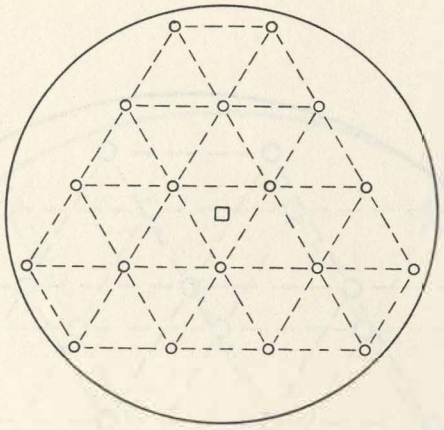

□—RADAR SITE
○—GAGE LOCATION
18 GAGES
S = 0.45 r

(Gage Pattern No. 12)

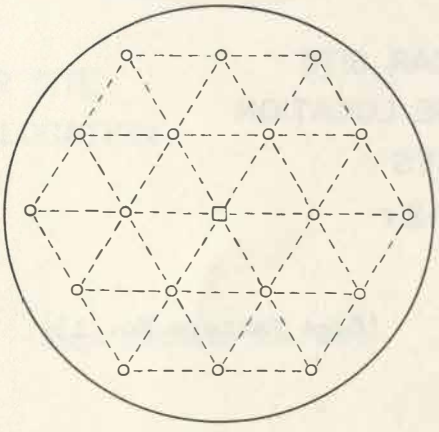

□—RADAR SITE
○—GAGE LOCATION
18 GAGES
S = 0.44 r

(Gage Pattern No. 3)

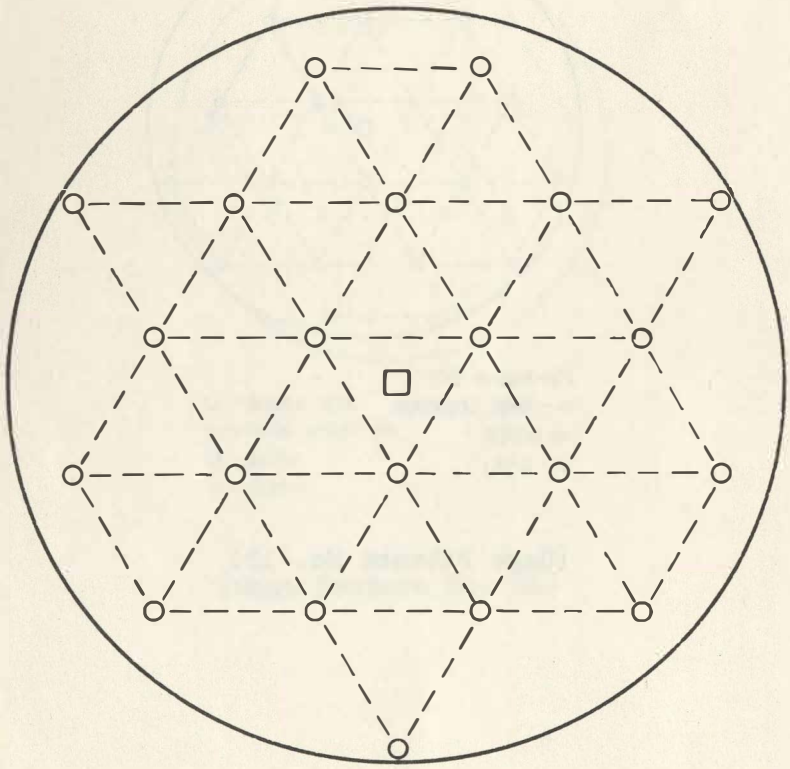

□—RADAR SITE

○—GAGE LOCATION

21 GAGES

S = 0.42 r

(Gage Pattern No. 13)

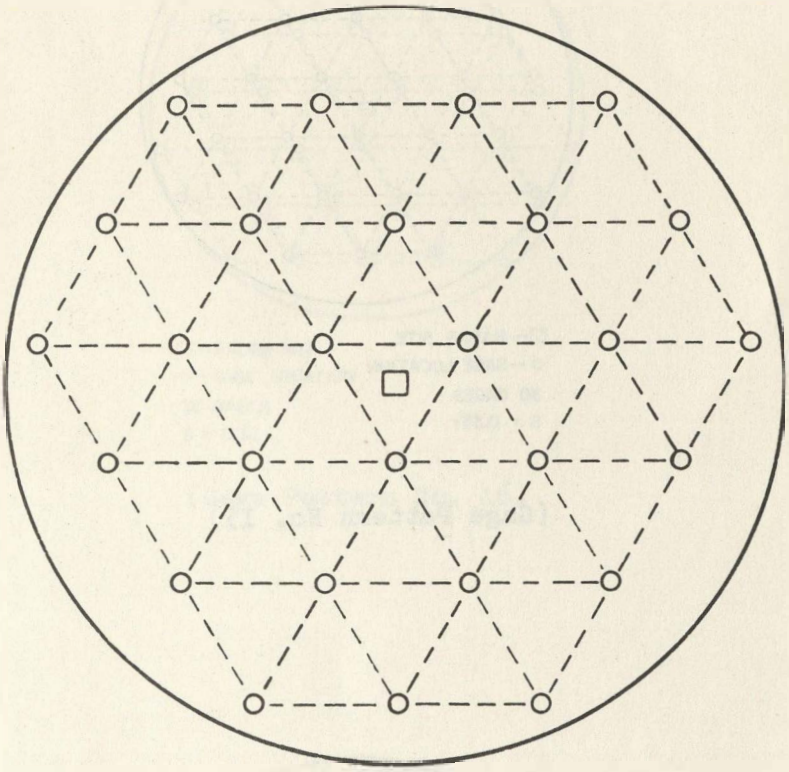

□—RADAR SITE

○—GAGE LOCATION

27 GAGES

S = 0.37 r

(Gage Pattern No. 14)

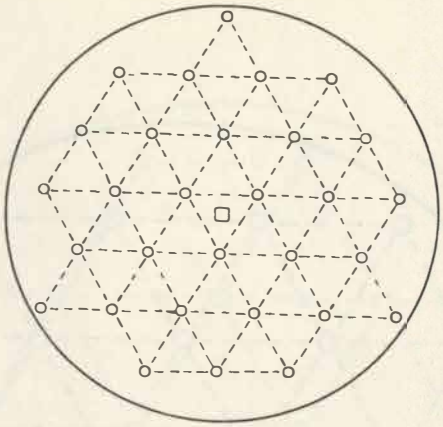

□—RADAR SITE
o—GAGE LOCATION
30 GAGES
S = 0.35r

(Gage Pattern No. 15)

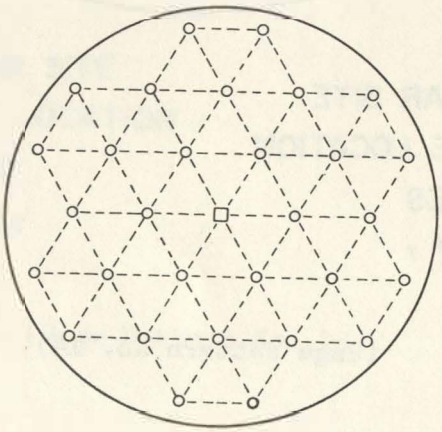

□—RADAR SITE
o—GAGE LOCATION
30 GAGES
S = 0.34 r

(Gage Pattern No. 4)

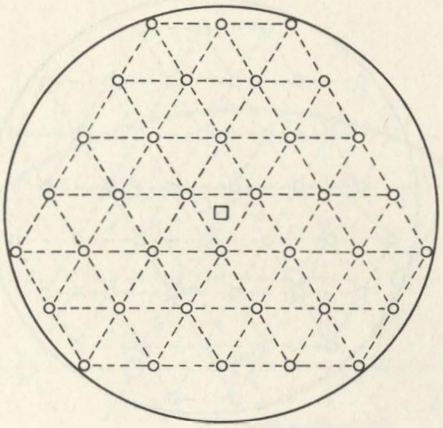

□—RADAR SITE
o—GAGE LOCATION
36 GAGES
S = 0.32 r

(Gage Pattern No. 16)

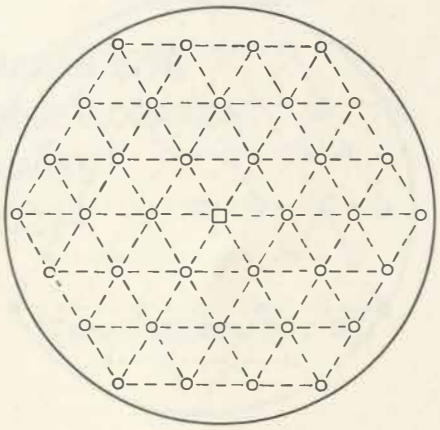

□—RADAR SITE
o—GAGE LOCATION
36 GAGES
S = 0.31 r

(Gage Pattern No. 5)

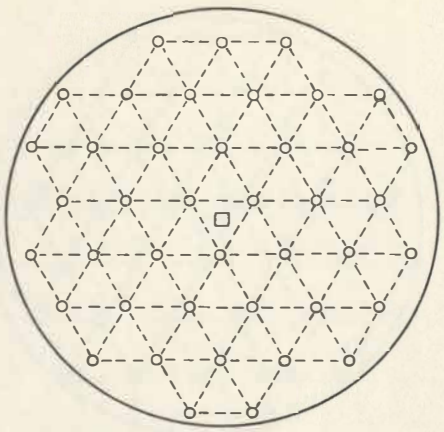

□—RADAR SITE
o—GAGE LOCATION
42 GAGES
S = 0.29r

(Gage Pattern No. 17)

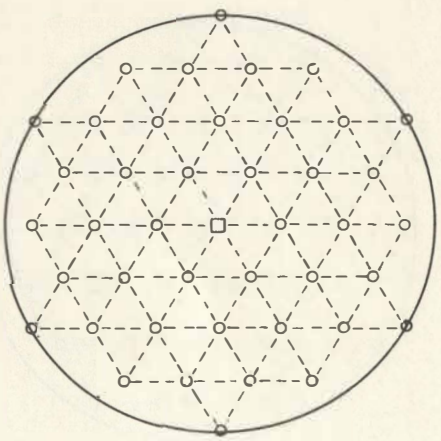

□—RADAR SITE
o—GAGE LOCATION
42 GAGES
S = 0.29r

(Gage Pattern No. 8)

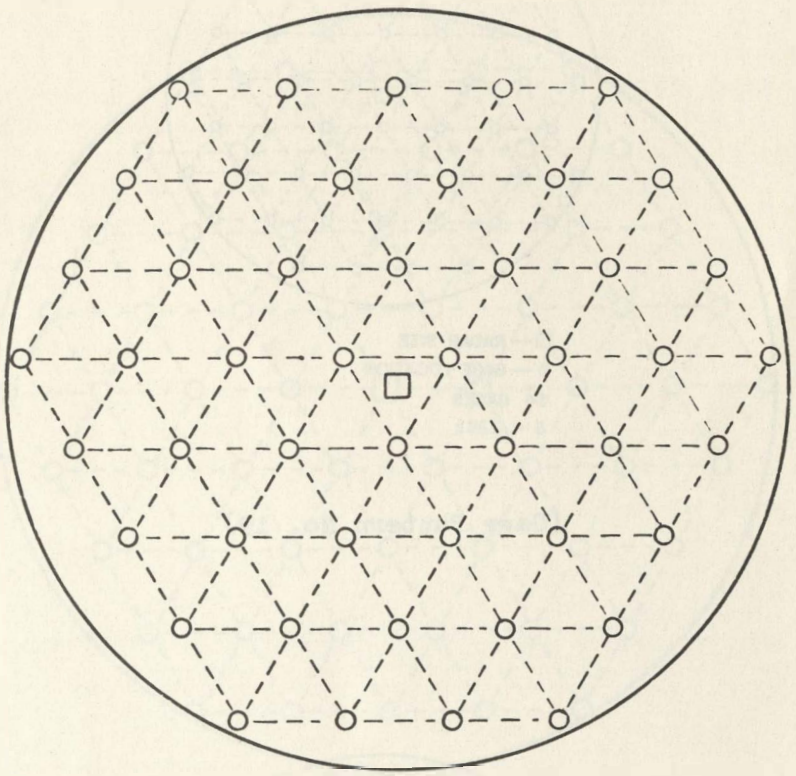

□—RADAR SITE

○—GAGE LOCATION

48 GAGES

S = 0.27r

(Gage Pattern No. 18)

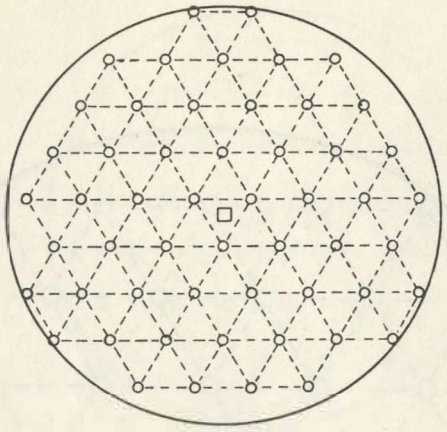

□ — RADAR SITE
o — GAGE LOCATION
54 GAGES
S = 0.26r

(Gage Pattern No. 19)

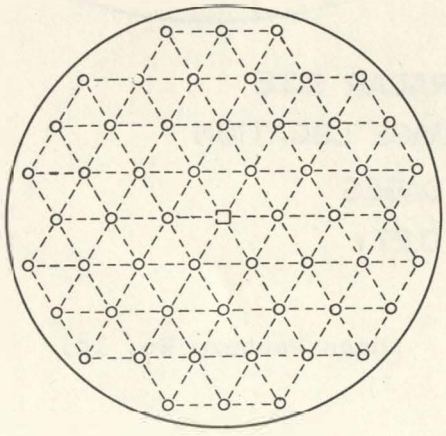

□ — RADAR SITE
o — GAGE LOCATION
54 GAGES
S = 0.26 r

(Gage Pattern No. 6)

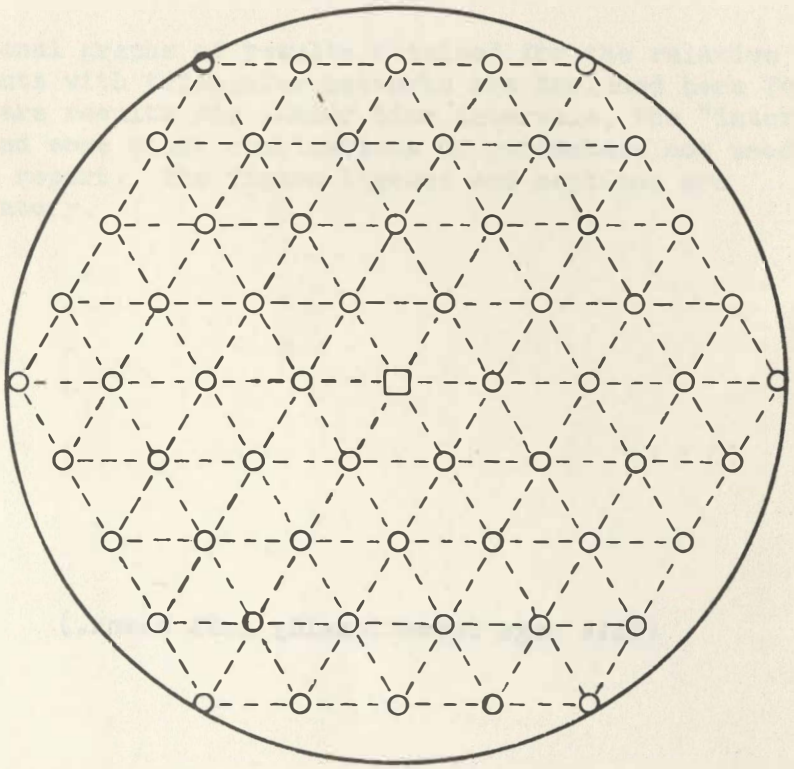

□—RADAR SITE

○—GAGE LOCATION

60—GAGES

S = 0.24 r

(Gage Pattern No. 7)

(This page intentionally left blank.)

# APPENDIX C

## Additional Results for Triangular Networks

Additional graphs of results obtained for the relative frequencies of gage events with triangular networks are included here for reference. Among them are results for 1-hour time intervals, the "intersection" networks, and some other combinations of parameters not used in the body of the report. The figure legends and captions are self-explanatory.

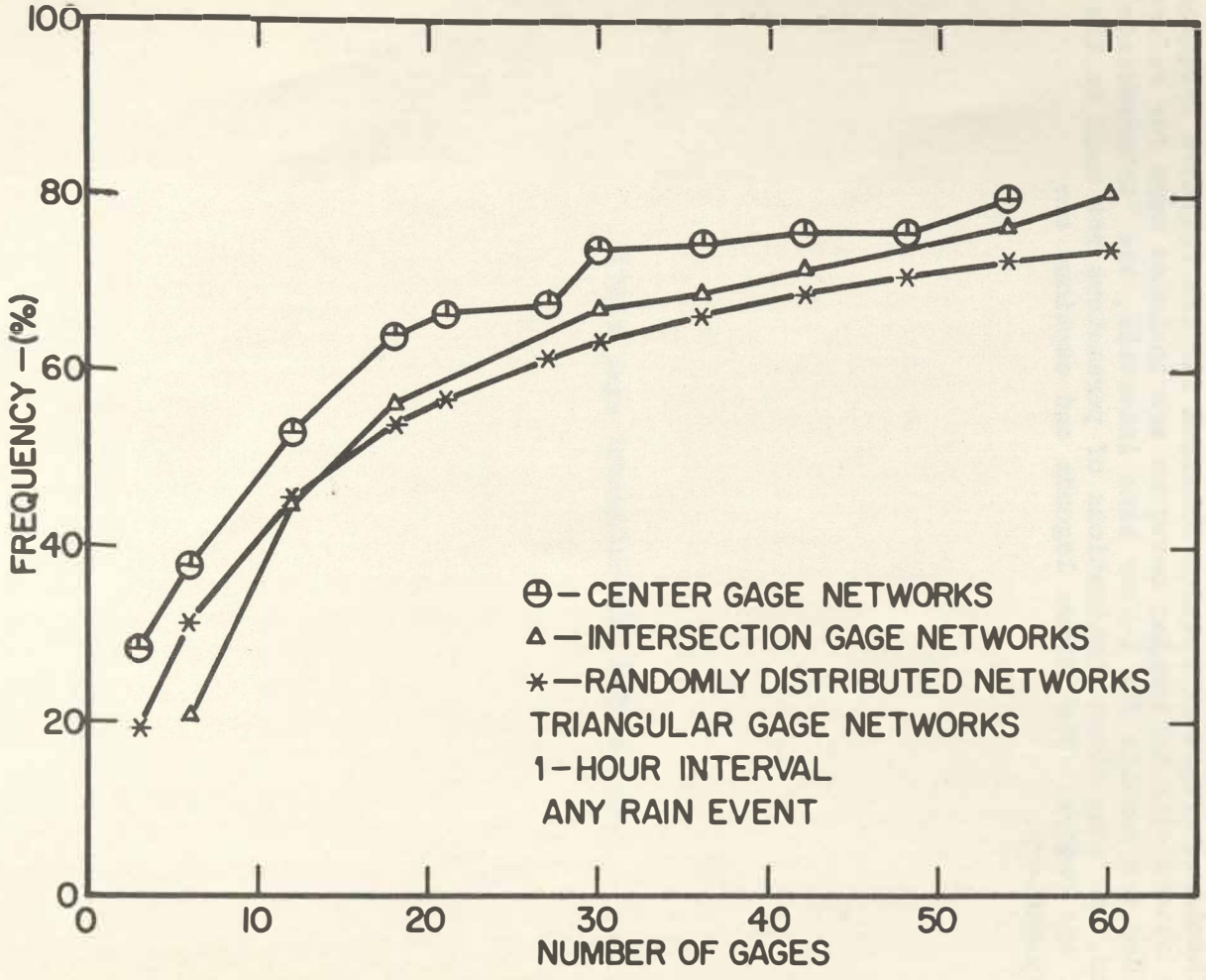
100
80
60
40
20
0
FREQUENCY – (%)
0
10
20
30
40
50
60
NUMBER OF GAGES
⊖ – CENTER GAGE NETWORKS
△ – INTERSECTION GAGE NETWORKS
* – RANDOMLY DISTRIBUTED NETWORKS
TRIANGULAR GAGE NETWORKS
1-HOUR INTERVAL
ANY RAIN EVENT

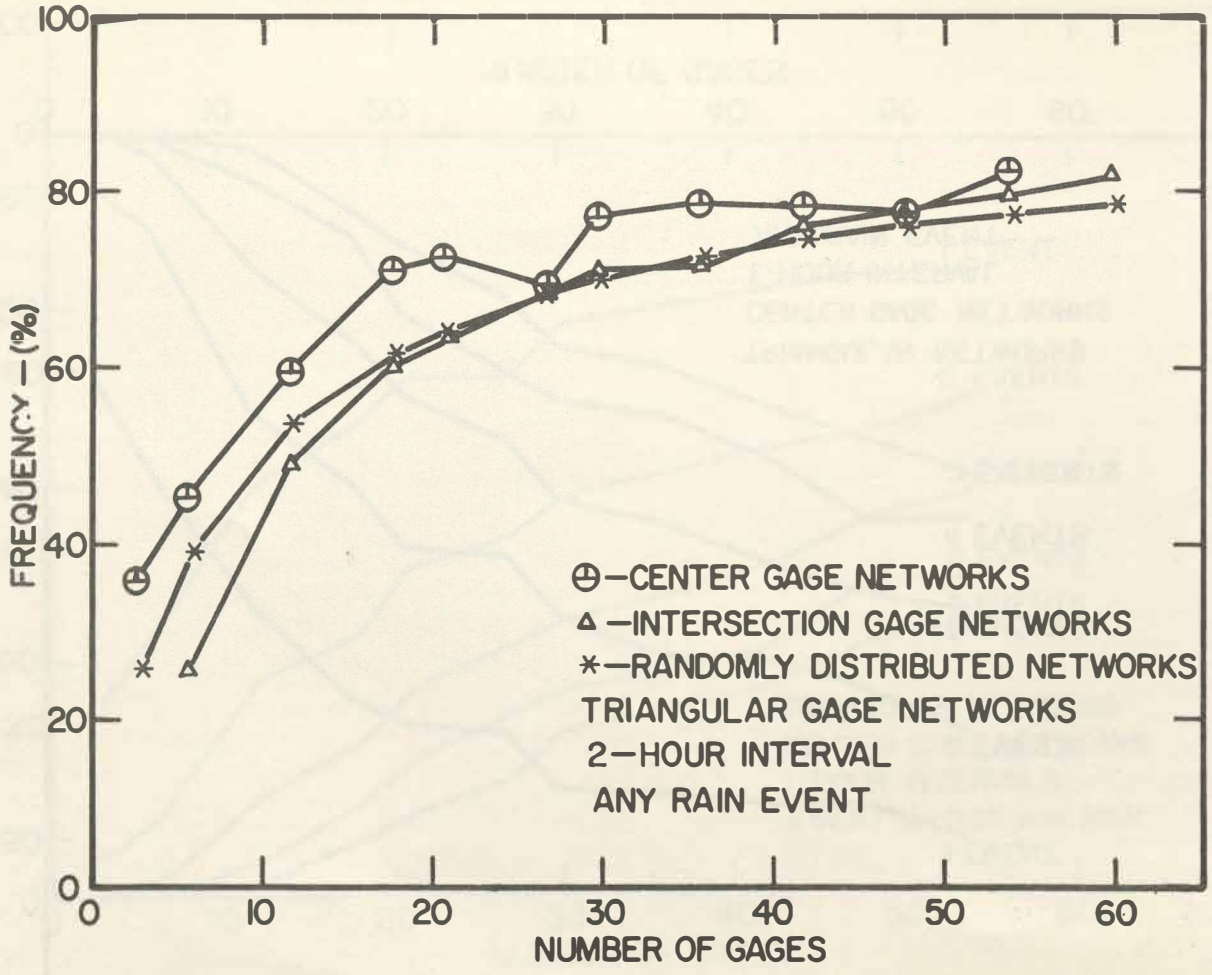
100
80
60
40
20
0
FREQUENCY — (%)
0
10
20
30
40
50
60
NUMBER OF GAGES
⊕—CENTER GAGE NETWORKS
△—INTERSECTION GAGE NETWORKS
*—RANDOMLY DISTRIBUTED NETWORKS
TRIANGULAR GAGE NETWORKS
2—HOUR INTERVAL
ANY RAIN EVENT

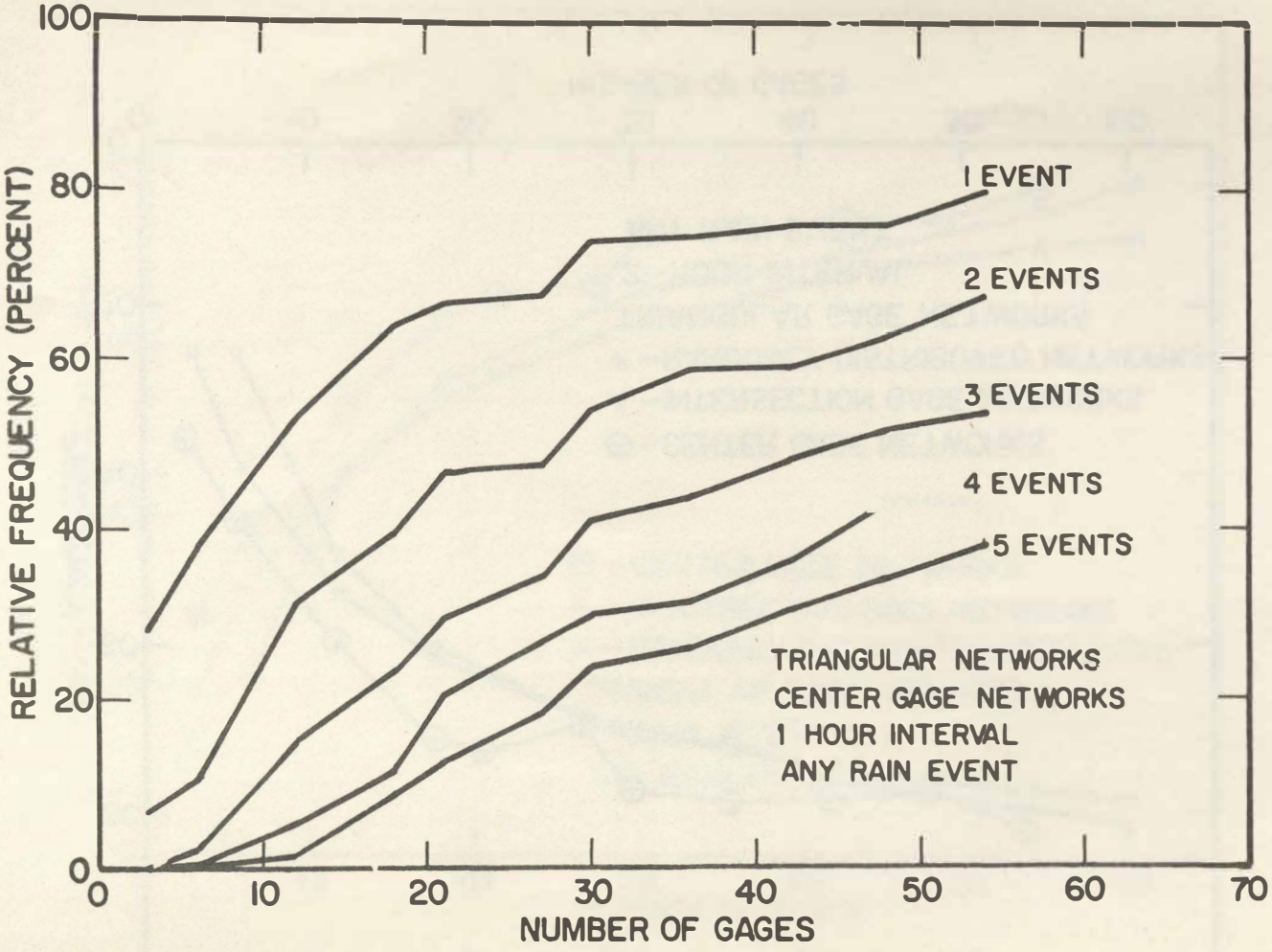
100
80
60
40
20
0
0
10
20
30
40
50
60
70
RELATIVE FREQUENCY (PERCENT)
NUMBER OF GAGES
1 EVENT
2 EVENTS
3 EVENTS
4 EVENTS
5 EVENTS
TRIANGULAR NETWORKS
CENTER GAGE NETWORKS
1 HOUR INTERVAL
ANY RAIN EVENT

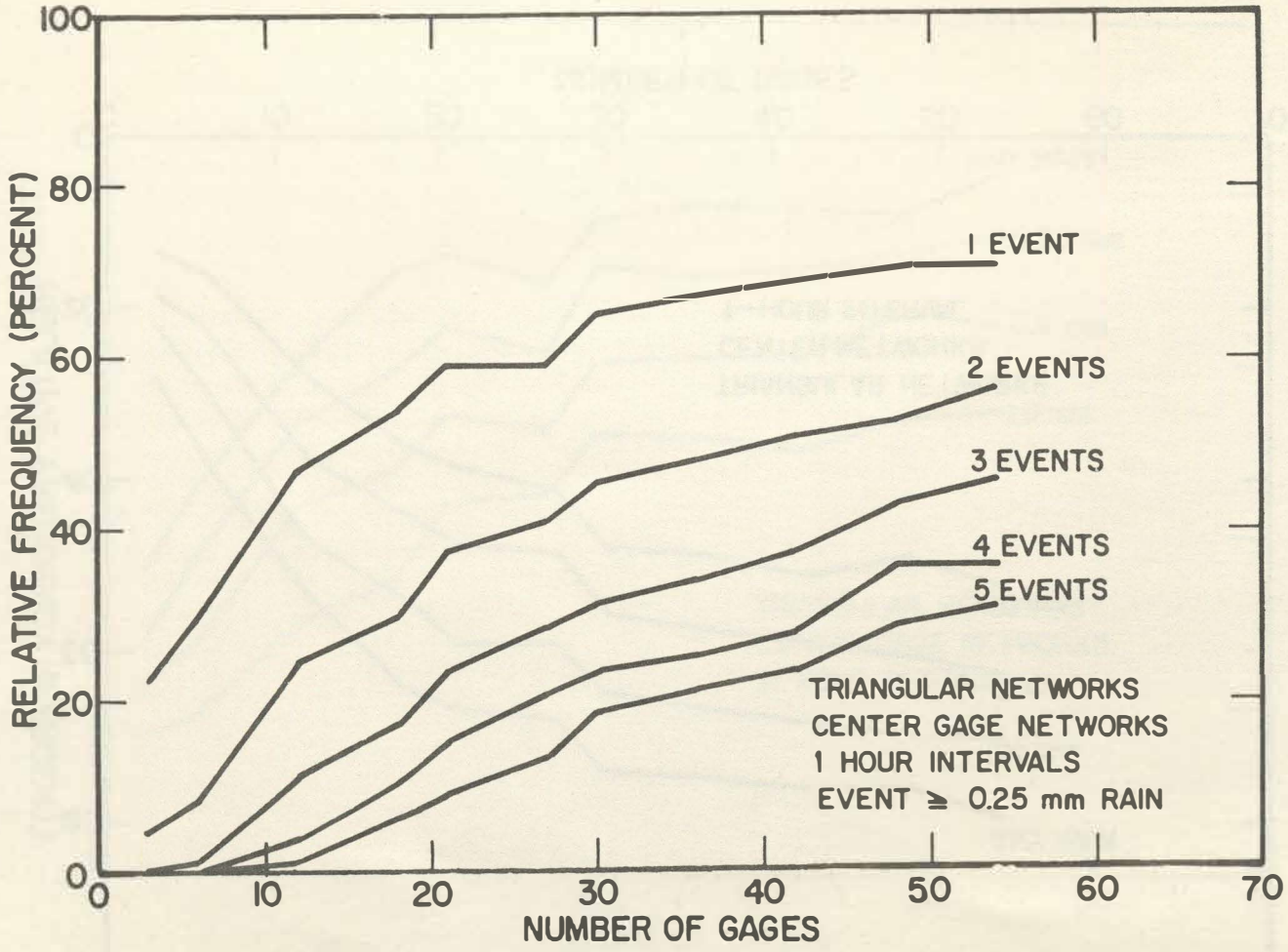
100
80
60
40
20
0
0
10
20
30
40
50
60
70
RELATIVE FREQUENCY (PERCENT)
NUMBER OF GAGES
1 EVENT
2 EVENTS
3 EVENTS
4 EVENTS
5 EVENTS
TRIANGULAR NETWORKS
CENTER GAGE NETWORKS
1 HOUR INTERVALS
EVENT ≥ 0.25 mm RAIN

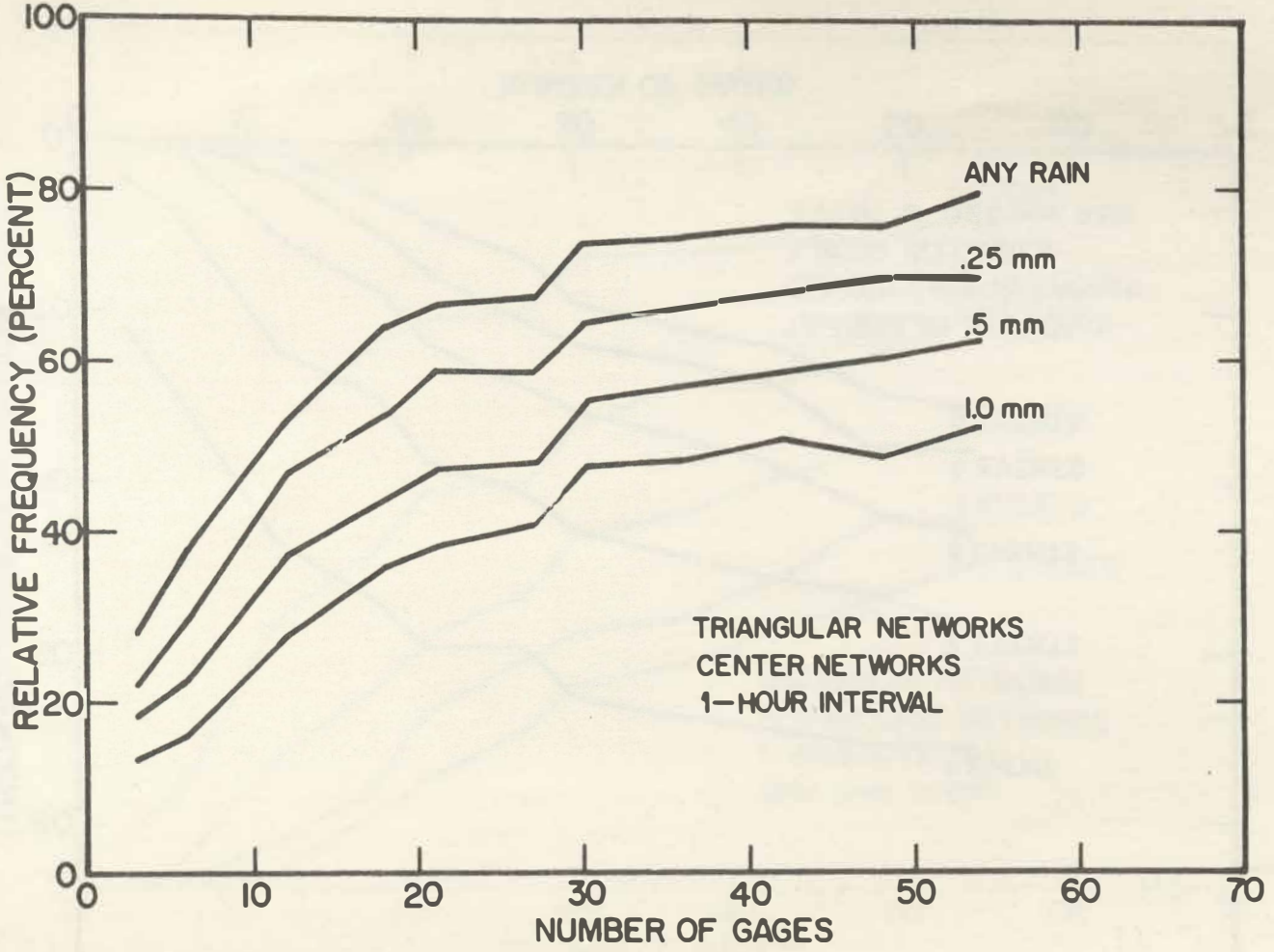
100
80
60
40
20
0
RELATIVE FREQUENCY (PERCENT)
0
10
20
30
40
50
60
70
NUMBER OF GAGES
ANY RAIN
.25 mm
.5 mm
1.0 mm
TRIANGULAR NETWORKS
CENTER NETWORKS
1-HOUR INTERVAL

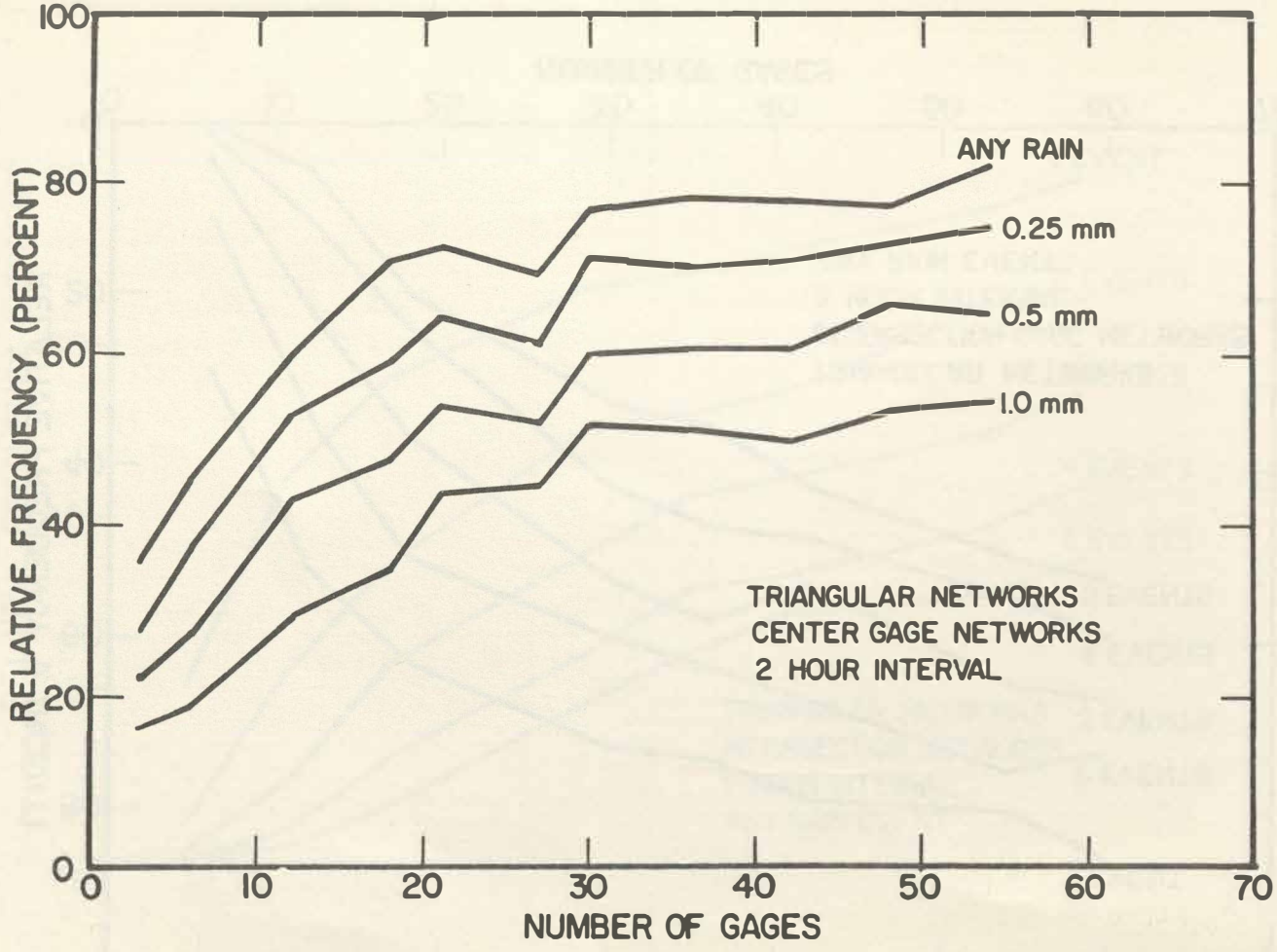
100
80
60
40
20
0
RELATIVE FREQUENCY (PERCENT)
ANY RAIN
0.25 mm
0.5 mm
1.0 mm
TRIANGULAR NETWORKS
CENTER GAGE NETWORKS
2 HOUR INTERVAL
0
10
20
30
40
50
60
70
NUMBER OF GAGES

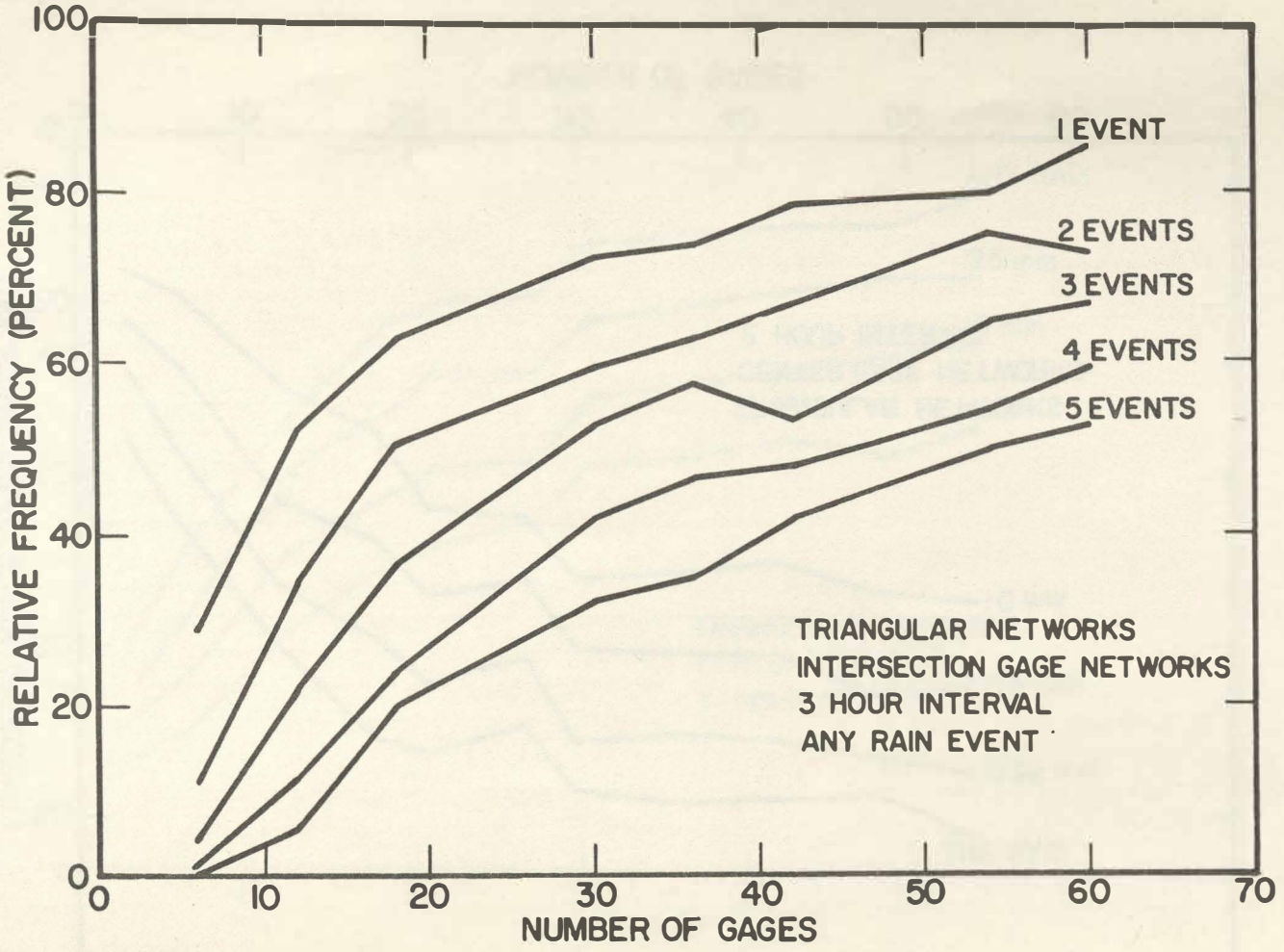
100
80
60
40
20
0
RELATIVE FREQUENCY (PERCENT)
0
10
20
30
40
50
60
70
NUMBER OF GAGES
1 EVENT
2 EVENTS
3 EVENTS
4 EVENTS
5 EVENTS
TRIANGULAR NETWORKS
INTERSECTION GAGE NETWORKS
3 HOUR INTERVAL
ANY RAIN EVENT

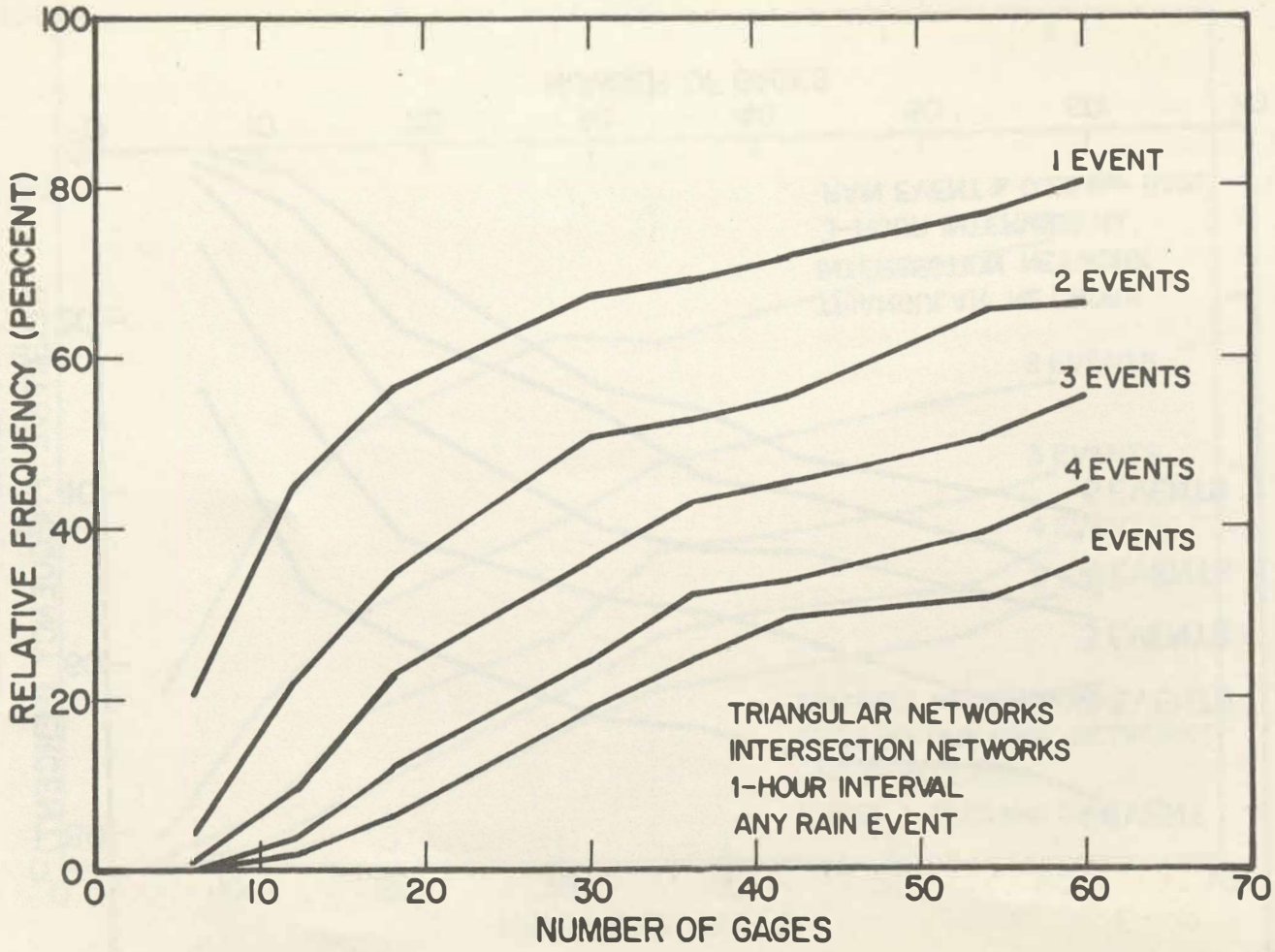
100
80
60
40
20
0
RELATIVE FREQUENCY (PERCENT)
0
10
20
30
40
50
60
70
NUMBER OF GAGES
1 EVENT
2 EVENTS
3 EVENTS
4 EVENTS
EVENTS
TRIANGULAR NETWORKS
INTERSECTION NETWORKS
1-HOUR INTERVAL
ANY RAIN EVENT

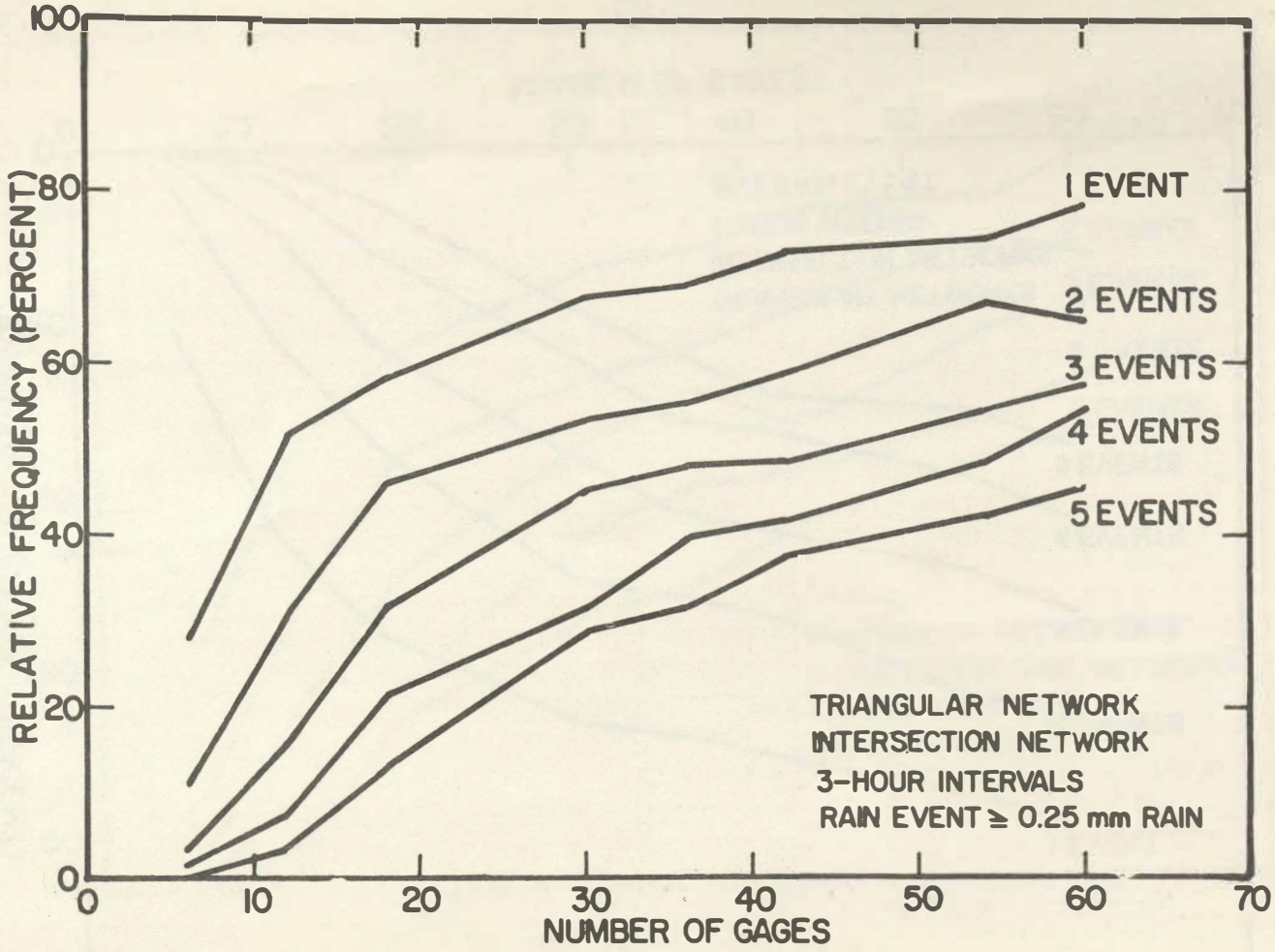
100
80
60
40
20
0
RELATIVE FREQUENCY (PERCENT)
0
10
20
30
40
50
60
70
NUMBER OF GAGES
1 EVENT
2 EVENTS
3 EVENTS
4 EVENTS
5 EVENTS
TRIANGULAR NETWORK
INTERSECTION NETWORK
3-HOUR INTERVALS
RAIN EVENT ≥ 0.25 mm RAIN

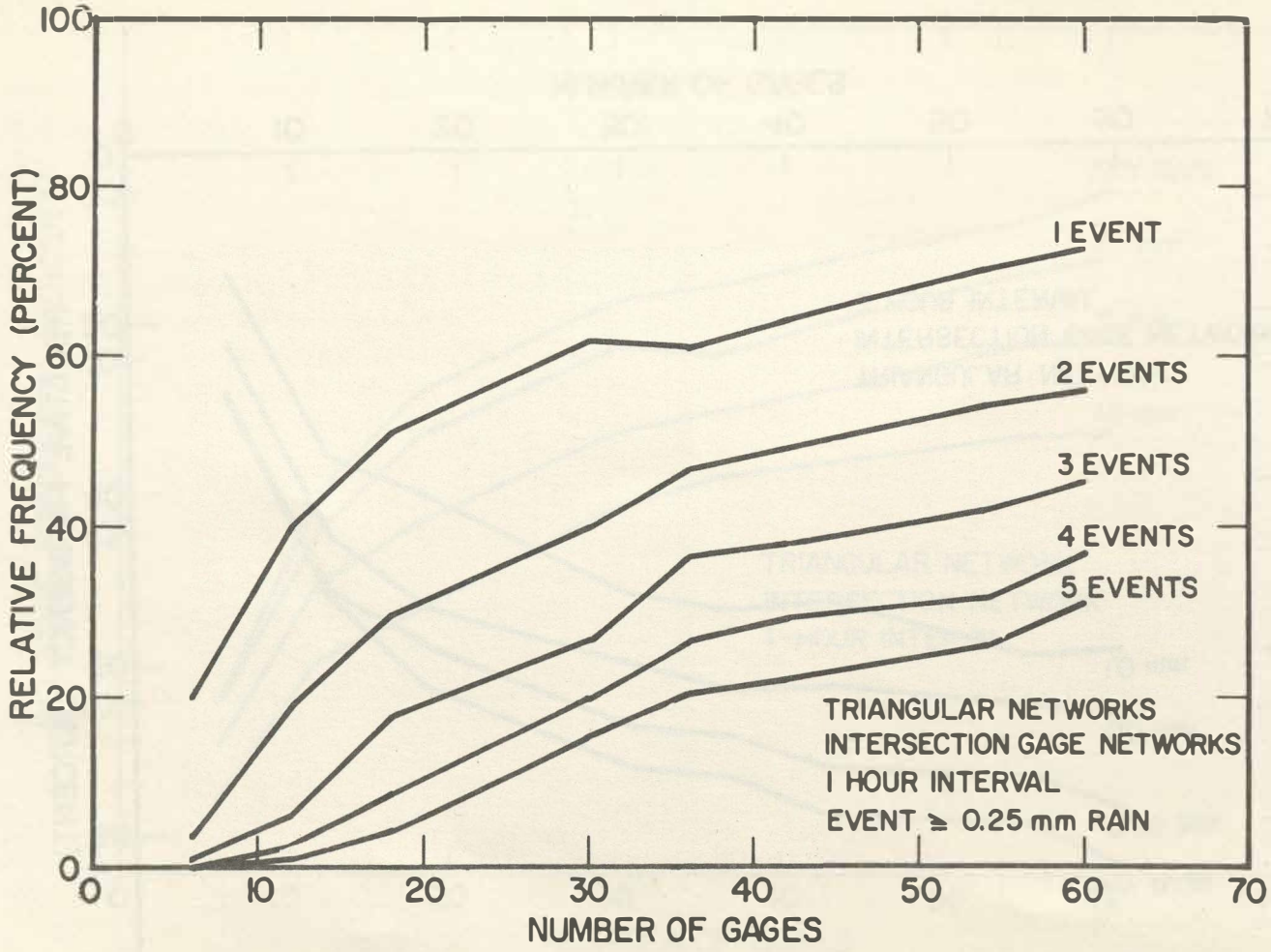
RELATIVE FREQUENCY (PERCENT)
100
80
60
40
20
0
0
10
20
30
40
50
60
70
NUMBER OF GAGES
1 EVENT
2 EVENTS
3 EVENTS
4 EVENTS
5 EVENTS
TRIANGULAR NETWORKS
INTERSECTION GAGE NETWORKS
1 HOUR INTERVAL
EVENT ≥ 0.25 mm RAIN

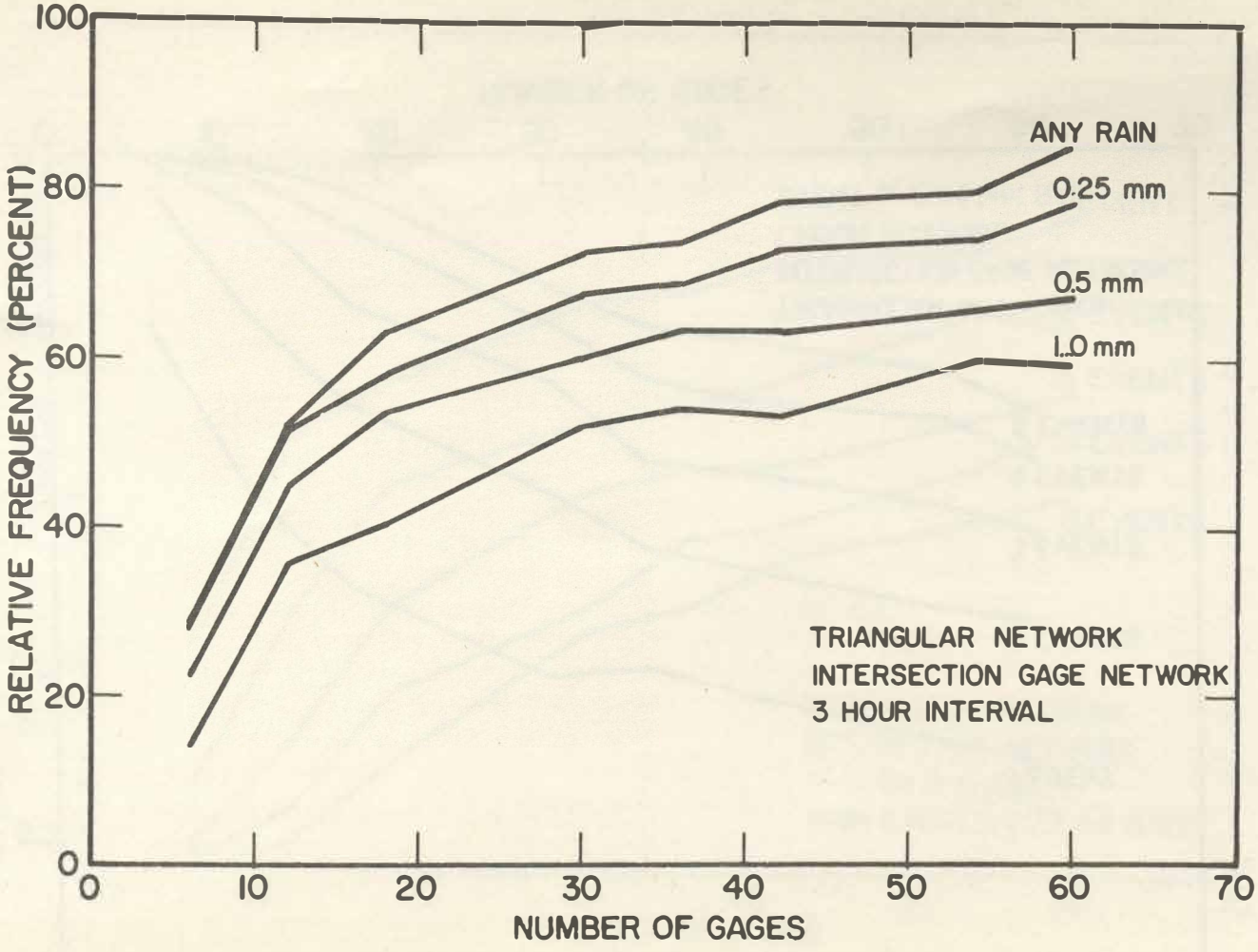
100
80
60
40
20
0
RELATIVE FREQUENCY (PERCENT)
0
10
20
30
40
50
60
70
NUMBER OF GAGES
ANY RAIN
0.25 mm
0.5 mm
1.0 mm
TRIANGULAR NETWORK
INTERSECTION GAGE NETWORK
3 HOUR INTERVAL

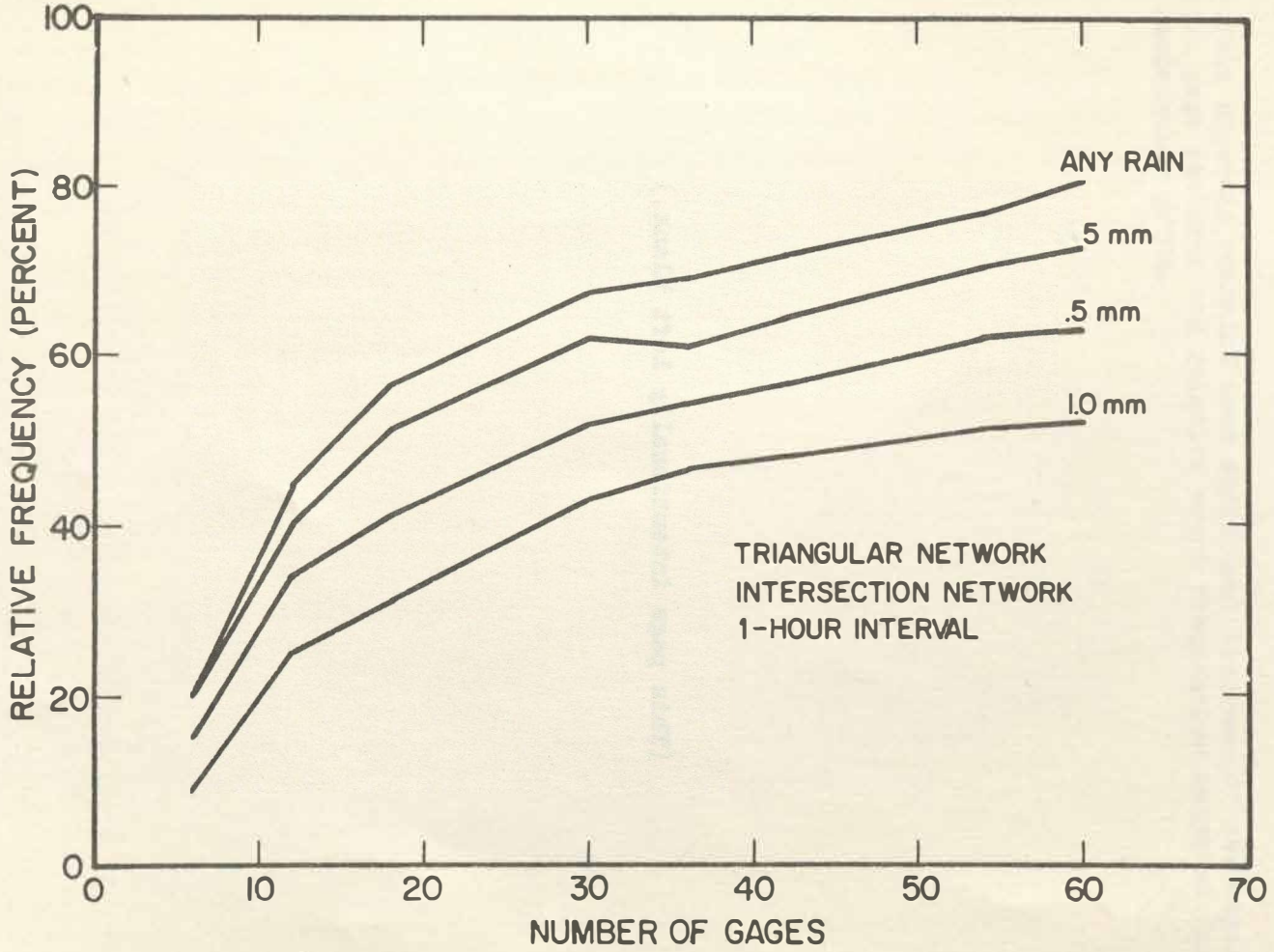
100
80
60
40
20
0
RELATIVE FREQUENCY (PERCENT)
0
10
20
30
40
50
60
70
NUMBER OF GAGES
ANY RAIN
5 mm
.5 mm
1.0 mm
TRIANGULAR NETWORK
INTERSECTION NETWORK
1-HOUR INTERVAL

(This page intentionally left blank.)

# APPENDIX D

## Graphs for Rectangular Networks

This appendix contains some additional diagrams of rectangular network gage patterns and relative event frequencies computed for the rectangular grids.

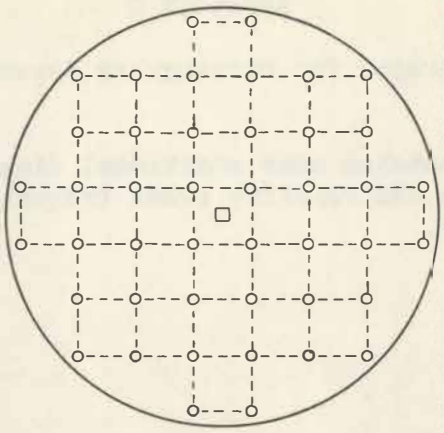

□ — RADAR SITE
○ — GAGE LOCATION
44 GAGES CENTERED
S = 0.27r

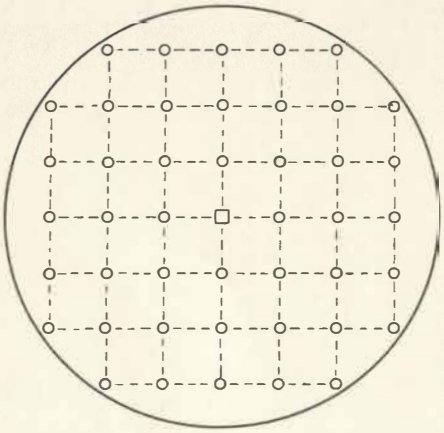

□ — RADAR SITE
○ — GAGE LOCATION
44 GAGES INTERSECTION
S = 0.27r

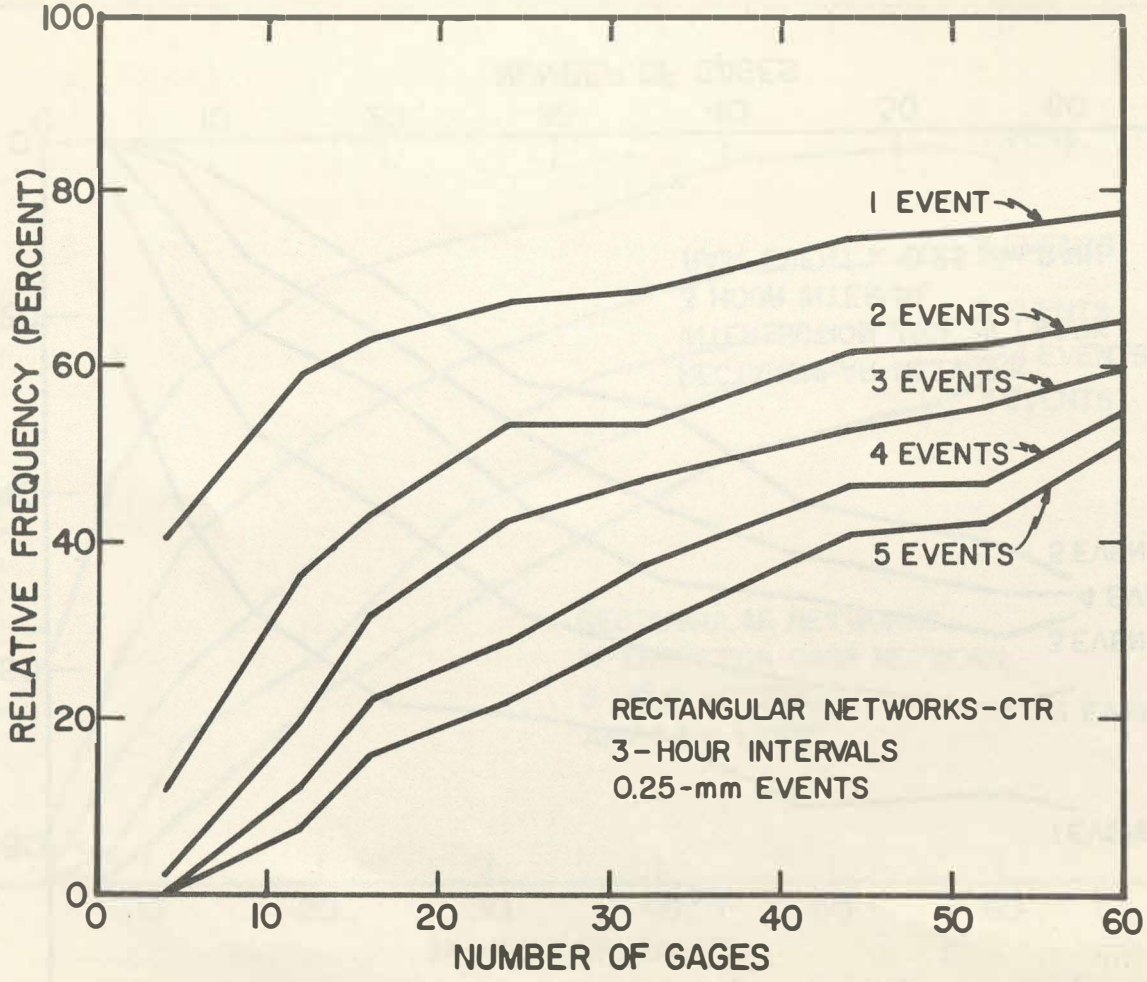
100
80
60
40
20
0
0
10
20
30
40
50
60
RELATIVE FREQUENCY (PERCENT)
NUMBER OF GAGES
1 EVENT
2 EVENTS
3 EVENTS
4 EVENTS
5 EVENTS
RECTANGULAR NETWORKS-CTR
3-HOUR INTERVALS
0.25-mm EVENTS

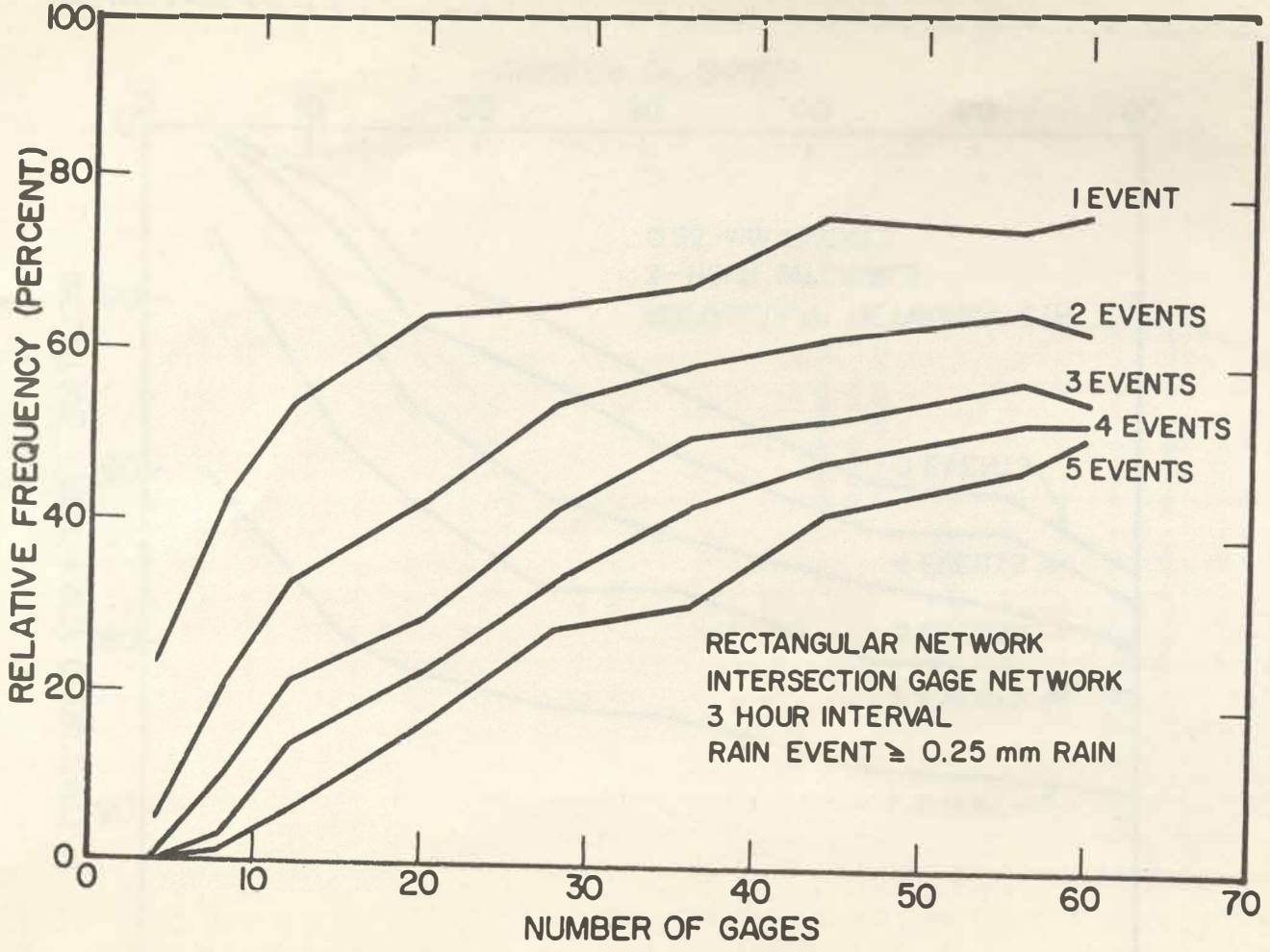
100
80
60
40
20
0
RELATIVE FREQUENCY (PERCENT)
0
10
20
30
40
50
60
70
NUMBER OF GAGES
1 EVENT
2 EVENTS
3 EVENTS
4 EVENTS
5 EVENTS
RECTANGULAR NETWORK
INTERSECTION GAGE NETWORK
3 HOUR INTERVAL
RAIN EVENT ≥ 0.25 mm RAIN

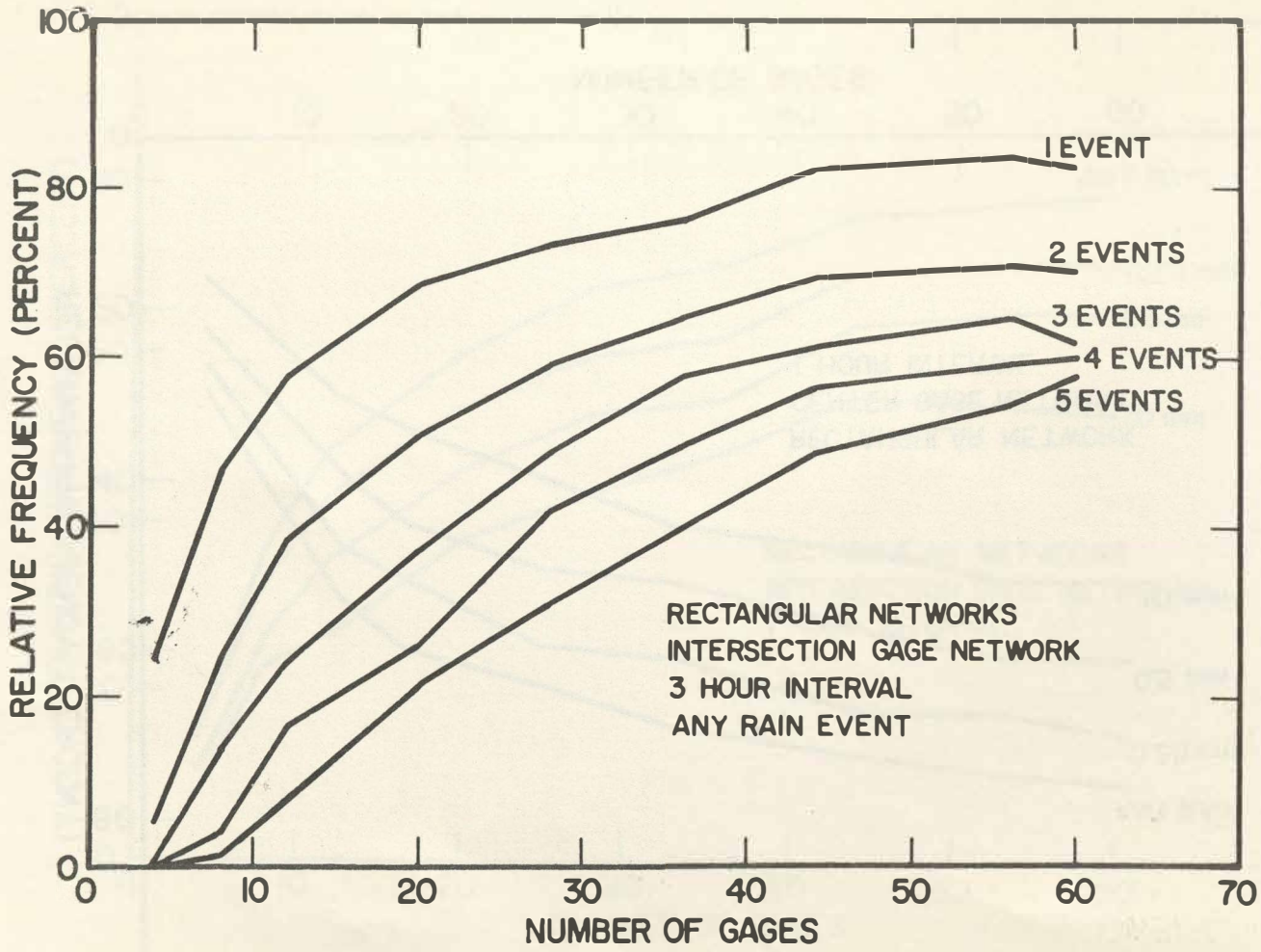
100
80
60
40
20
0
RELATIVE FREQUENCY (PERCENT)
0
10
20
30
40
50
60
70
NUMBER OF GAGES
1 EVENT
2 EVENTS
3 EVENTS
4 EVENTS
5 EVENTS
RECTANGULAR NETWORKS
INTERSECTION GAGE NETWORK
3 HOUR INTERVAL
ANY RAIN EVENT

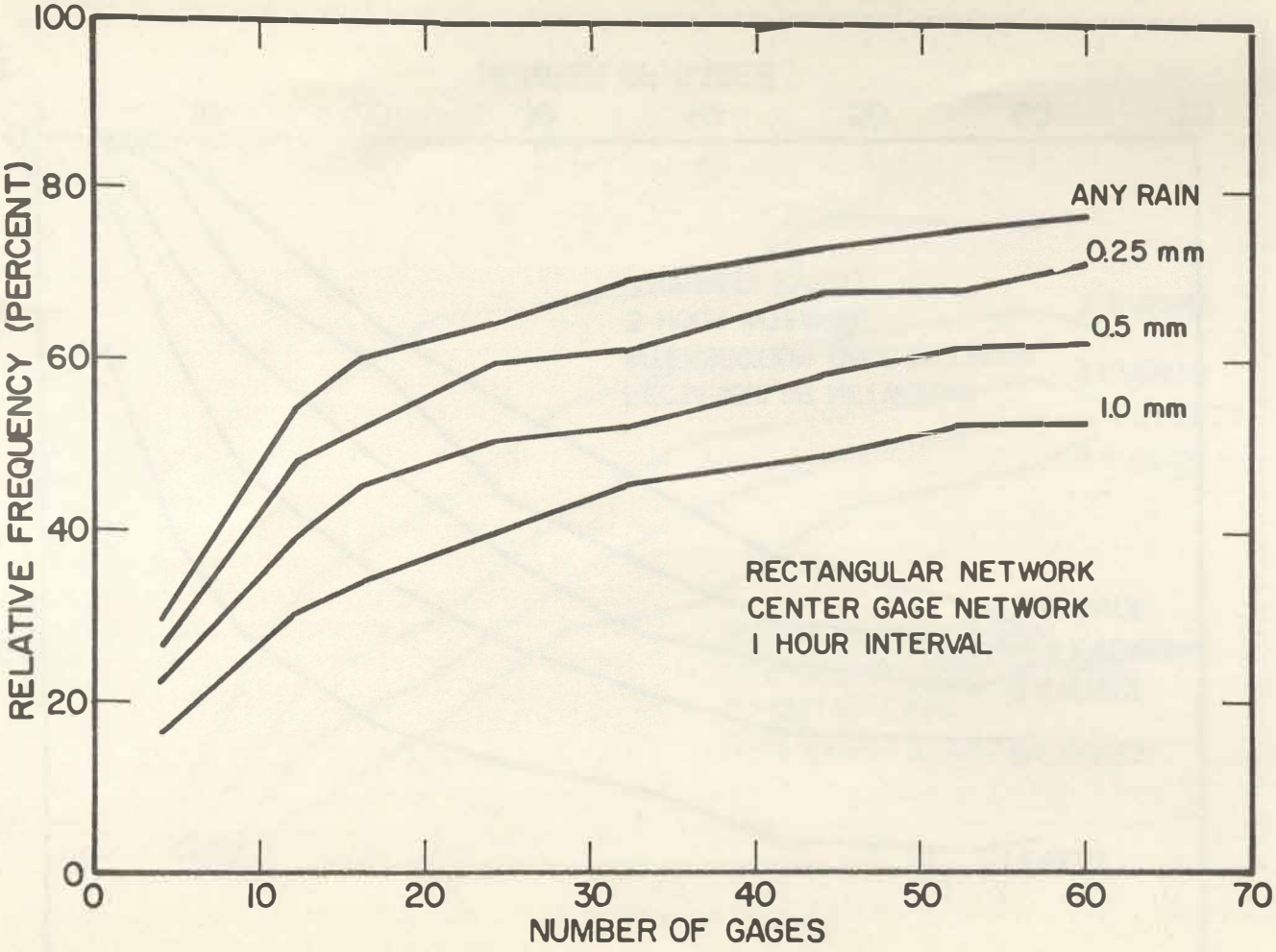
100
80
60
40
20
0
RELATIVE FREQUENCY (PERCENT)
0
10
20
30
40
50
60
70
NUMBER OF GAGES
ANY RAIN
0.25 mm
0.5 mm
1.0 mm
RECTANGULAR NETWORK
CENTER GAGE NETWORK
1 HOUR INTERVAL

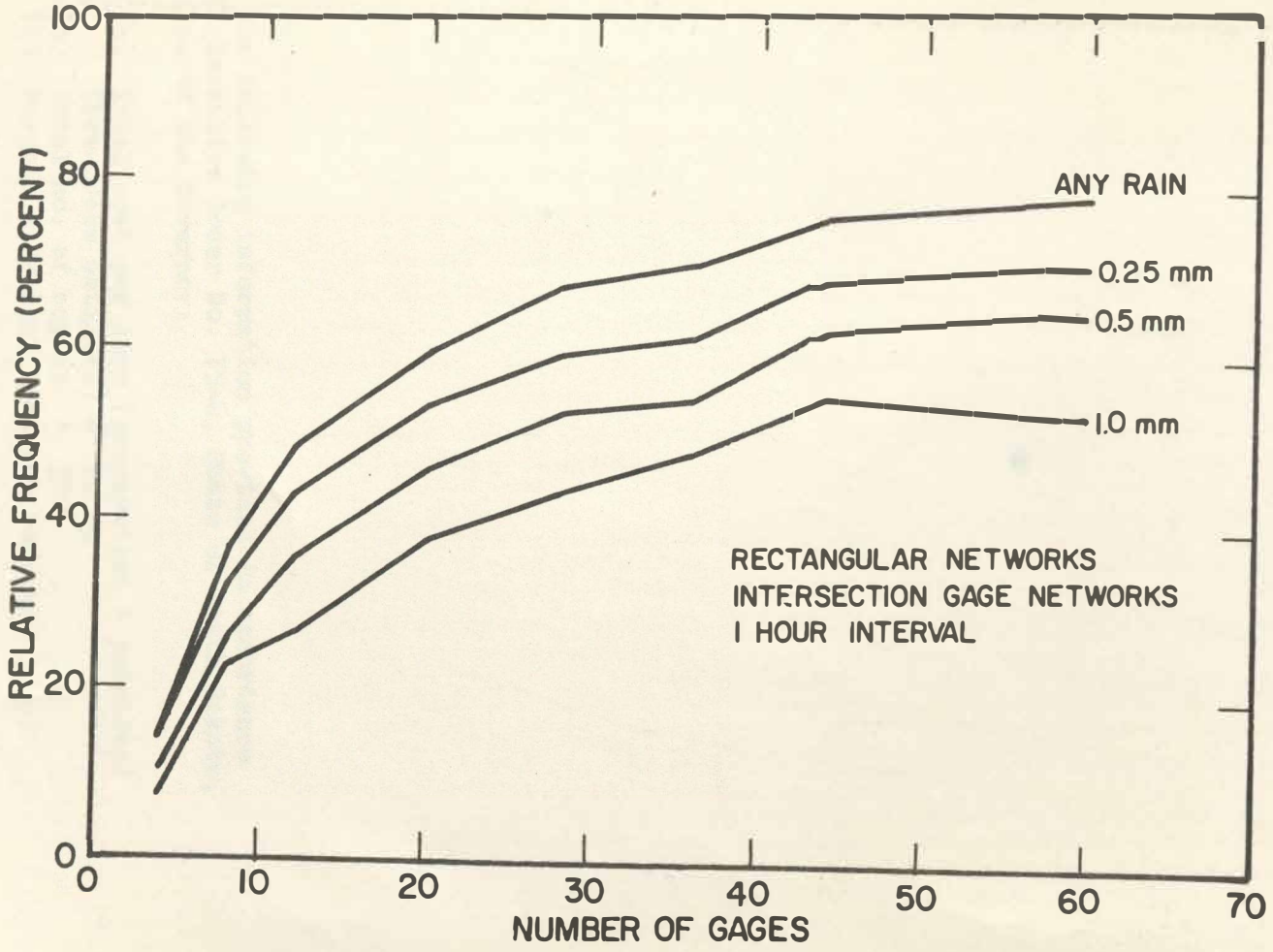
100
80
60
40
20
0
RELATIVE FREQUENCY (PERCENT)
0
10
20
30
40
50
60
70
NUMBER OF GAGES
ANY RAIN
0.25 mm
0.5 mm
1.0 mm
RECTANGULAR NETWORKS
INTERSECTION GAGE NETWORKS
1 HOUR INTERVAL

The following information provided in accordance with Executive Order No. 75-6, State of South Dakota, Office of the Governor:

(a) Total cost per copy (preparation & printing) (Pre-press estimate) = $2.09
(b) Total no. of copies = 300
(c) Purpose = Present research results